

Synthesis and Characterization of BPA-free Polyesters by Incorporating a Semi-rigid Cyclobutanediol Monomer

Rahul K. Shahni,[†] Micah Mabin,[†] Zhihan Wang,[‡] Muneer Shaik,[†] Angel Ugrinov,[§] and Qianli Rick Chu^{*,†}

[†]Department of Chemistry, University of North Dakota, Grand Forks, ND 58202, USA; [‡]Department of Physical Sciences, Eastern New Mexico University, Portales, NM 88130, USA; [§]Department of Chemistry and Biochemistry, North Dakota State University, Fargo, ND 58102, USA. *Correspondence and requests for materials should be addressed to Q. R. Chu. (email: chu@chem.und.edu)

Table of Contents

1. Experiment setup.....	4
1.1 Reaction setup for synthesis of CBDA-1.....	4
1.2 Synthesis of CBDO-1 based polyesters	5
2. Crystal Data.....	6
2.1 SXRD structure and data of CBDO-1.....	6
2.2 Conformation of cyclobutane ring and crystal packing of CBDO-1.....	7
3. Spectral Data.....	8
3.1 ¹ H and D ₂ O exchange NMR spectra of CBDO-1 in CDCl ₃ at room temperature....	8
3.2 ¹³ C NMR spectrum of CBDO-1 in CDCl ₃ at room temperature.....	9
3.3 DEPT 45, 90 and 135 spectra of CBDO-1 in CDCl ₃ at room temperature.....	10
3.4 High resolution mass spectrometry of CBDO-1.....	11
3.5 FT-IR spectrum of CBDO-1 using ATR detector.....	12
3.6 ¹ H and ¹³ C exchange NMR spectra of PCBO in CDCl ₃ at room temperature.....	13
3.7 COSY and CH-correlation spectra of PCBO in CDCl ₃ at room temperature.....	14
3.8 FT-IR spectrum of PCBO using ATR detector.....	15
3.9 ¹ H and ¹³ C exchange NMR spectra of PCB _M in CDCl ₃ at room temperature.....	16

3.10 COSY and CH-correlation spectra of PCBM in CDCl ₃ at room temperature.....	17
3.11 FT-IR spectrum of PCBM using ATR detector.....	18
3.12 ¹ H and ¹³ C exchange NMR spectra of PCBS in CDCl ₃ at room temperature.....	19
3.13 COSY and CH-correlation spectra of PCBS in CDCl ₃ at room temperature.....	20
3.14 FT-IR spectrum of PCBS using ATR detector.....	21
3.15 ¹ H and ¹³ C exchange NMR spectra of PCBG in CDCl ₃ at room temperature.....	22
3.16 COSY and CH-correlation spectra of PCBG in CDCl ₃ at room temperature.....	23
3.17 FT-IR spectrum of PCBG using ATR detector.....	24
3.18 ¹ H and ¹³ C exchange NMR spectra of PCBA in CDCl ₃ at room temperature.....	25
3.19 COSY and CH-correlation spectra of PCBA in CDCl ₃ at room temperature.....	26
3.20 FT-IR spectrum of PCBA using ATR detector.....	27
3.21 ¹ H and ¹³ C exchange NMR spectra of PCBT in CDCl ₃ at room temperature.....	28
3.22 COSY and CH-correlation spectra of PCBT in CDCl ₃ at room temperature.....	29
3.23 FT-IR spectrum of PCBT using ATR detector.....	30
3.24 ¹ H and ¹³ C exchange NMR spectra of PCBF in CDCl ₃ at room temperature.....	31
3.25 COSY and CH-correlation spectra of PCBF in CDCl ₃ at room temperature.....	32
3.26 FT-IR spectrum of PCBF using ATR detector.....	33
3.27 ¹ H and ¹³ C NMR spectra of PCBC in CDCl ₃ at room temperature.....	34
3.28 COSY and CH-correlation spectra of PCBC in CDCl ₃ at room temperature.....	35
3.29 FT-IR spectrum of PCBC using ATR detector.....	36
3.30 MALDI-TOF-MS spectrum of PCBS.....	37
3.31 MALDI-TOF-MS spectrum of PCBT.....	38
3.32 MALDI-TOF-MS spectrum of PCBF.....	39

3.33 MALDI-TOF-MS spectrum of PCBC.....	40
4. Thermo-physical data of some known polyesters compared with the CBPs.....	41
5. Molecular weight data obtained by using GPC & DOSY.....	41
5.1 Retention time of commercially available PS and PMMA using GPC.....	42
5.2 PS calibration curve data and figure for M_w prediction.....	42
5.3 2-D DOSY spectra of PCBA in $CDCl_3$	43
5.4 Exemplary signal intensity decay curve for PCBA.....	44

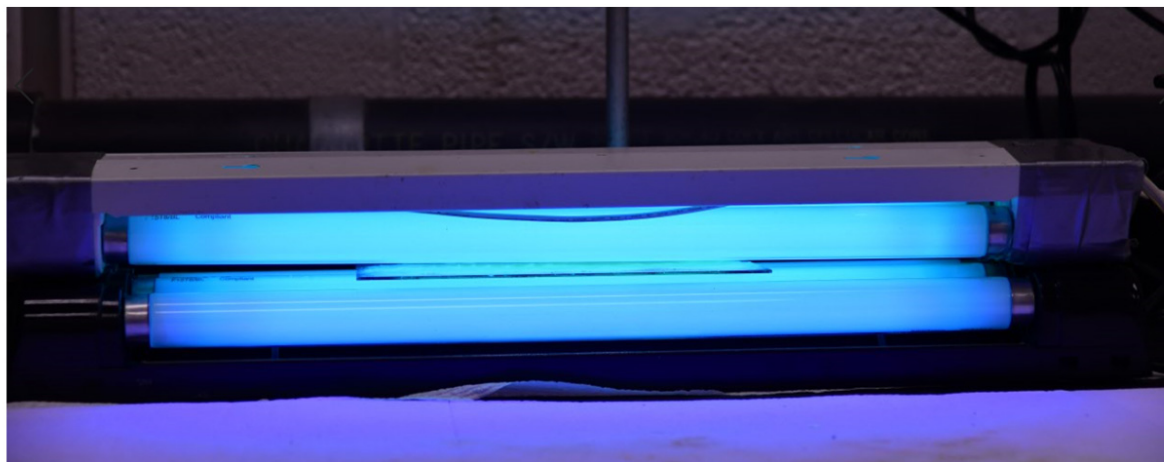


Figure S1. Setup for synthesis of CBDA-1 in the solid state

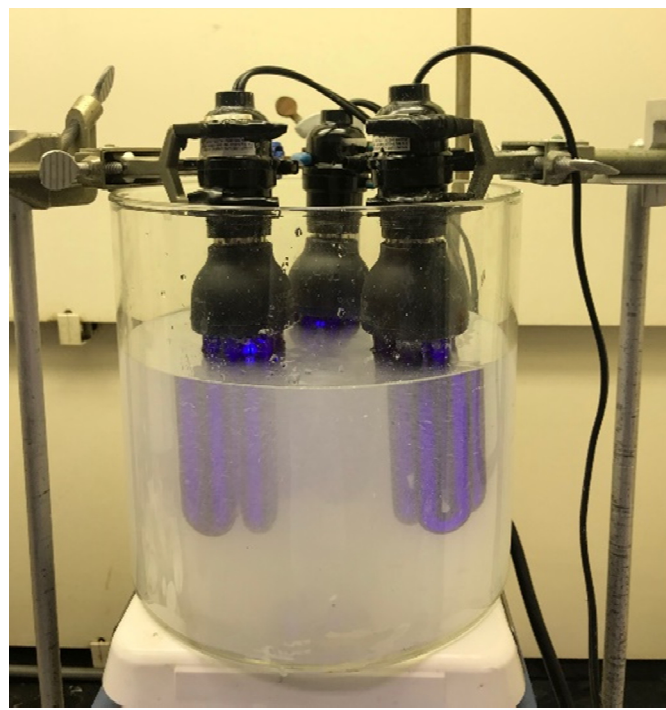


Figure S2. Setup for synthesis of CBDA-1 in brine slurry*

* To ensure that the brine was as transparent as possible, 25 mL water was added into the brine before the reaction and each day during the slurry photoreaction.

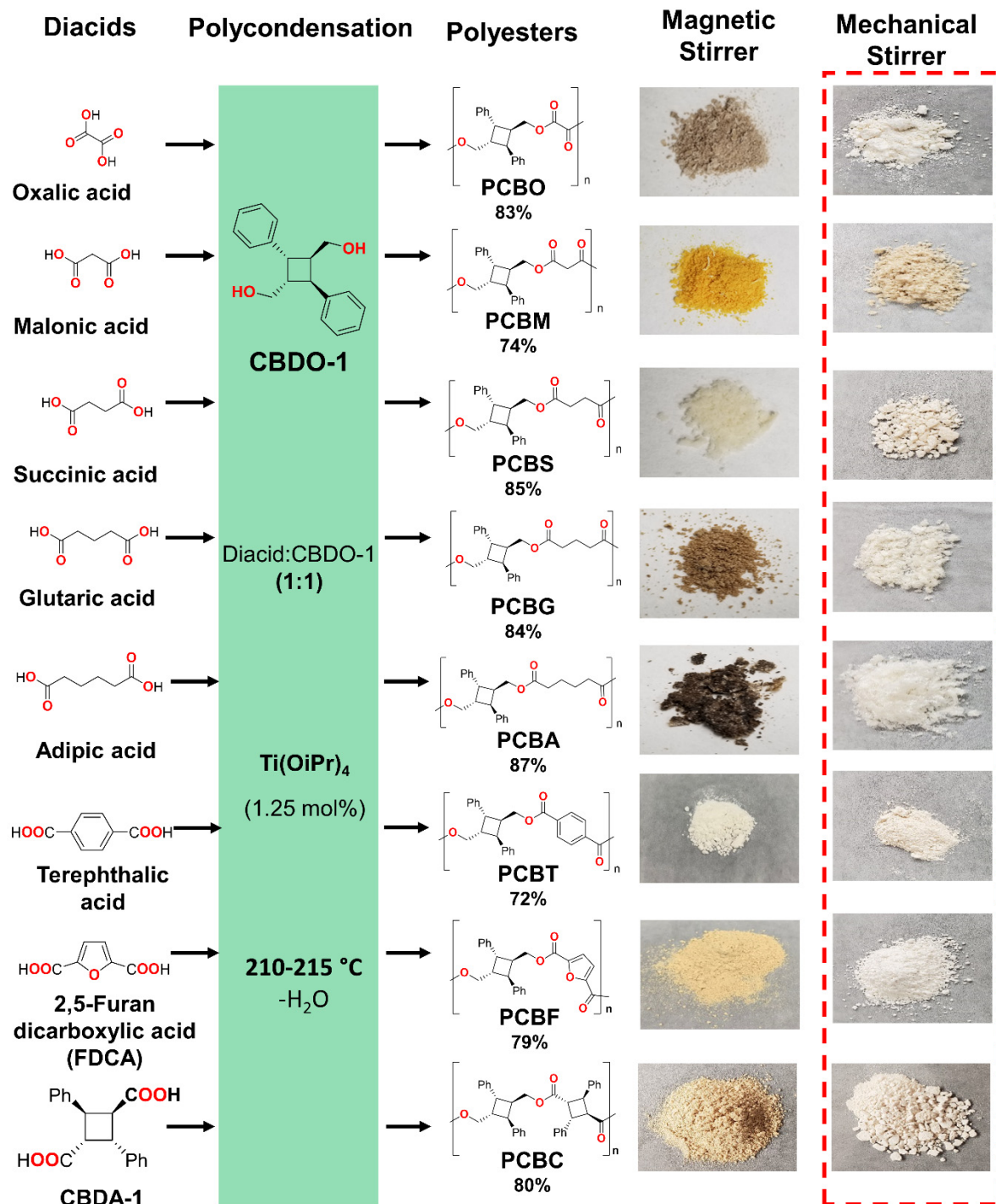
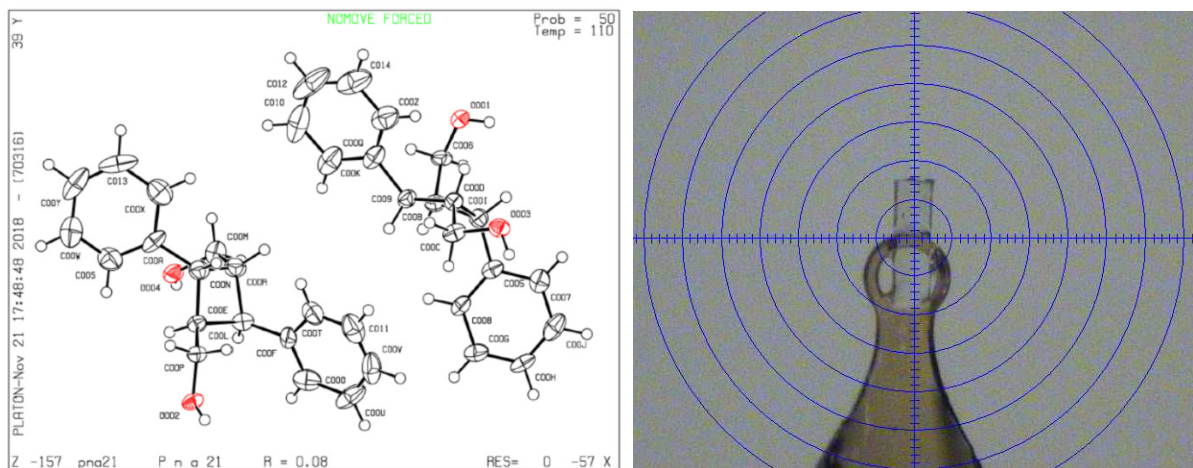


Figure S3. Synthesis of CBDO-1 based polyesters. Showing the color difference by using magnetic stirrer and external mechanical stirrer.

X-ray crystal structure and data of CBDO-1



CBDO-1	Data
CCDC #	1949075
Formula	C36 H40 O4
FW	536.68
Crystal Size [mm]	0.06 x 0.121 x 0.375
Crystal_system	orthorhombic
Space Group, Z	Pna ₂ ₁
a (Å)	17.9616 (7)
b (Å)	7.6761 (3)
c (Å)	21.5205(9)
α (°)	90
β (°)	90
γ (°)	90
V (Å ³)	2967.1(2)
Temp. (K)	110(2)
ρcalc [g/cm ³]	1.201
μ [mm ⁻¹]	0.604
Radiation Type	CuK\alpha
F(000)	1152
No of measured refl.	73145
of independent refl.	5263
No of refl. (I ≥ 2σ)	4930
R1/wR2 (I ≥ 2σ) [%]	7.82 /20.40
R1/wR2 (all data) [%]	8.25 /20.71

Conformation of cyclobutane ring and crystal packing of CBDO-1

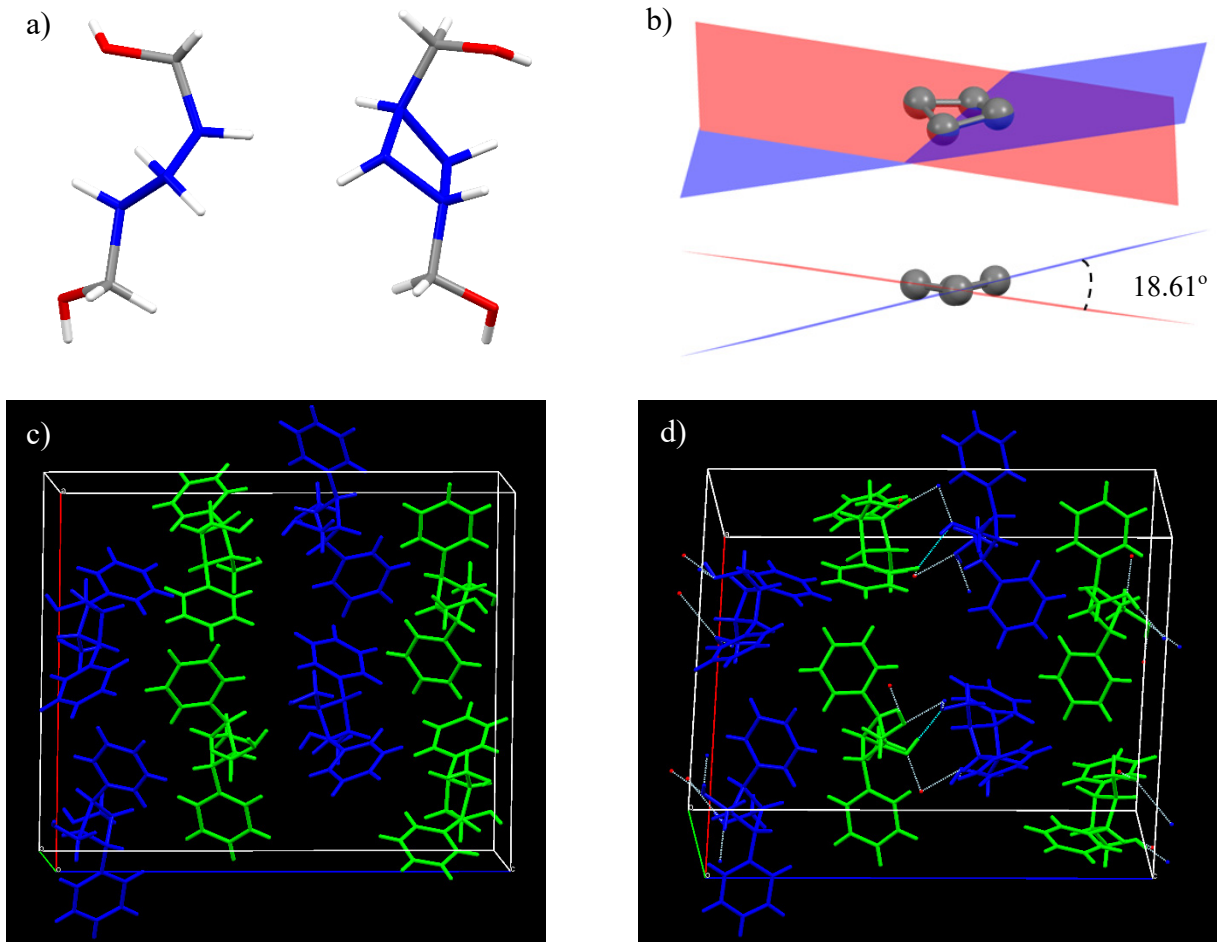


Figure S4. a) Two CBDO-1 molecules in the asymmetric unit cell (cyclobutane moiety highlighted in blue and the phenyl groups are omitted for clarity); b) Conformation of a cyclobutane ring in the crystal: The puckered cyclobutane ring of CBDO-1 with an angle of 18.61° , and the other one is 22.02° as shown in Figure 2 of the manuscript; c) The packing of CBDO-1 in crystal (In the unit cell, the molecules with the same symmetry equivalence are shown in the same color.); d) The packing of CBDO-1 in crystal with the hydrogen bonds shown in dash blue lines.

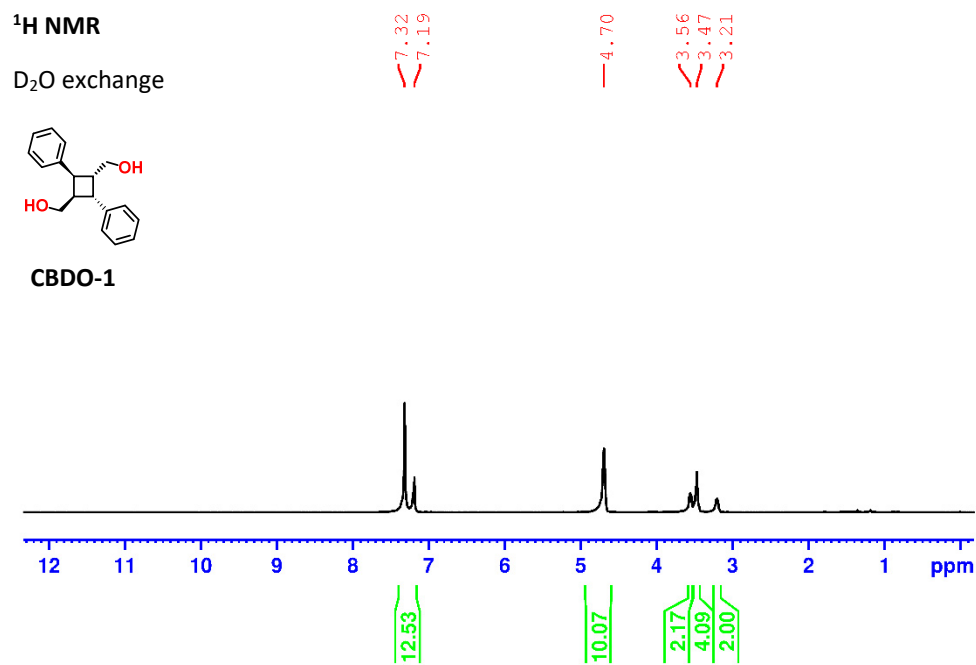
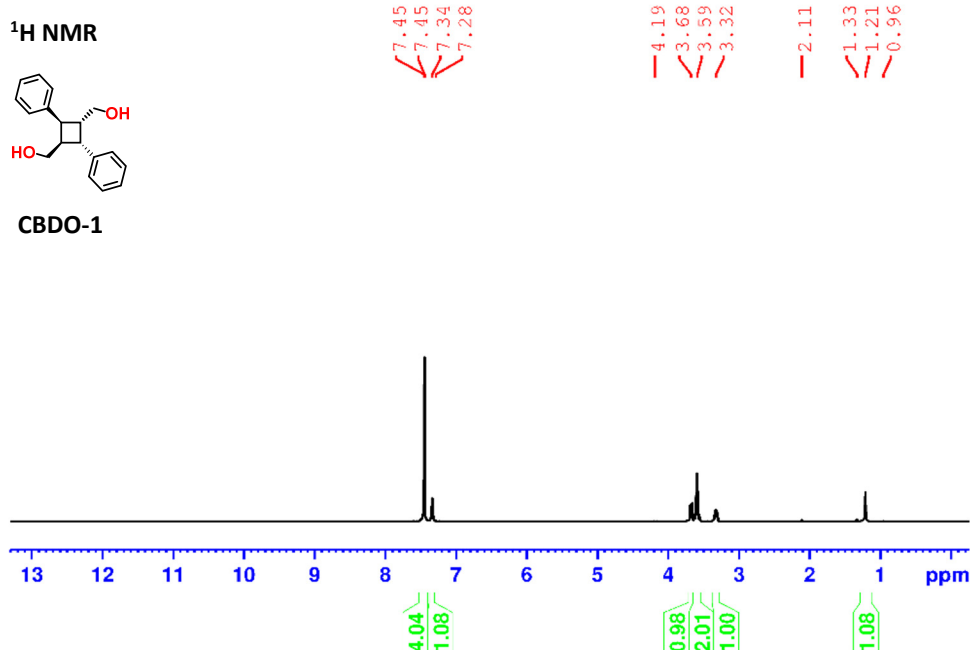


Figure S5. ¹H and D₂O exchange NMR spectra of **CBDO-1** in CDCl₃ at room temperature.

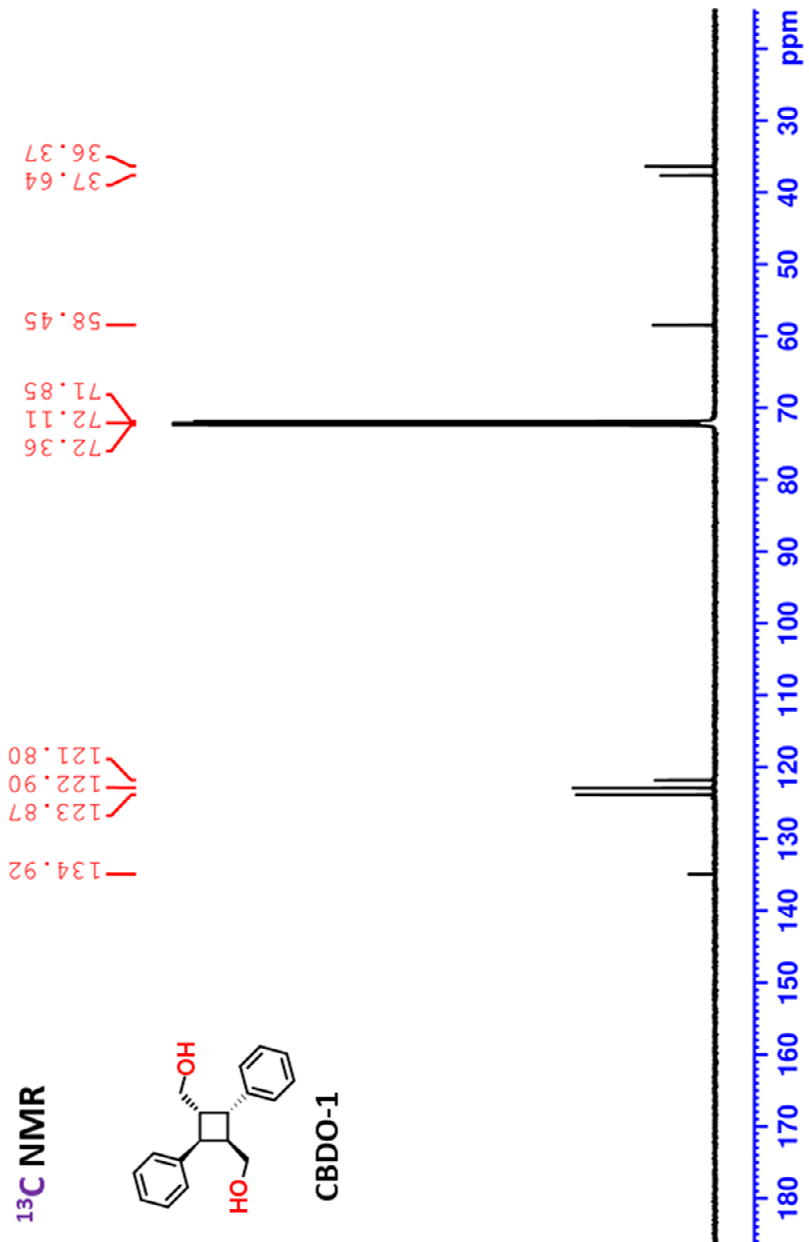


Figure S6. ¹³C NMR spectrum of **CBDO-1** in CDCl₃ at room temperature.

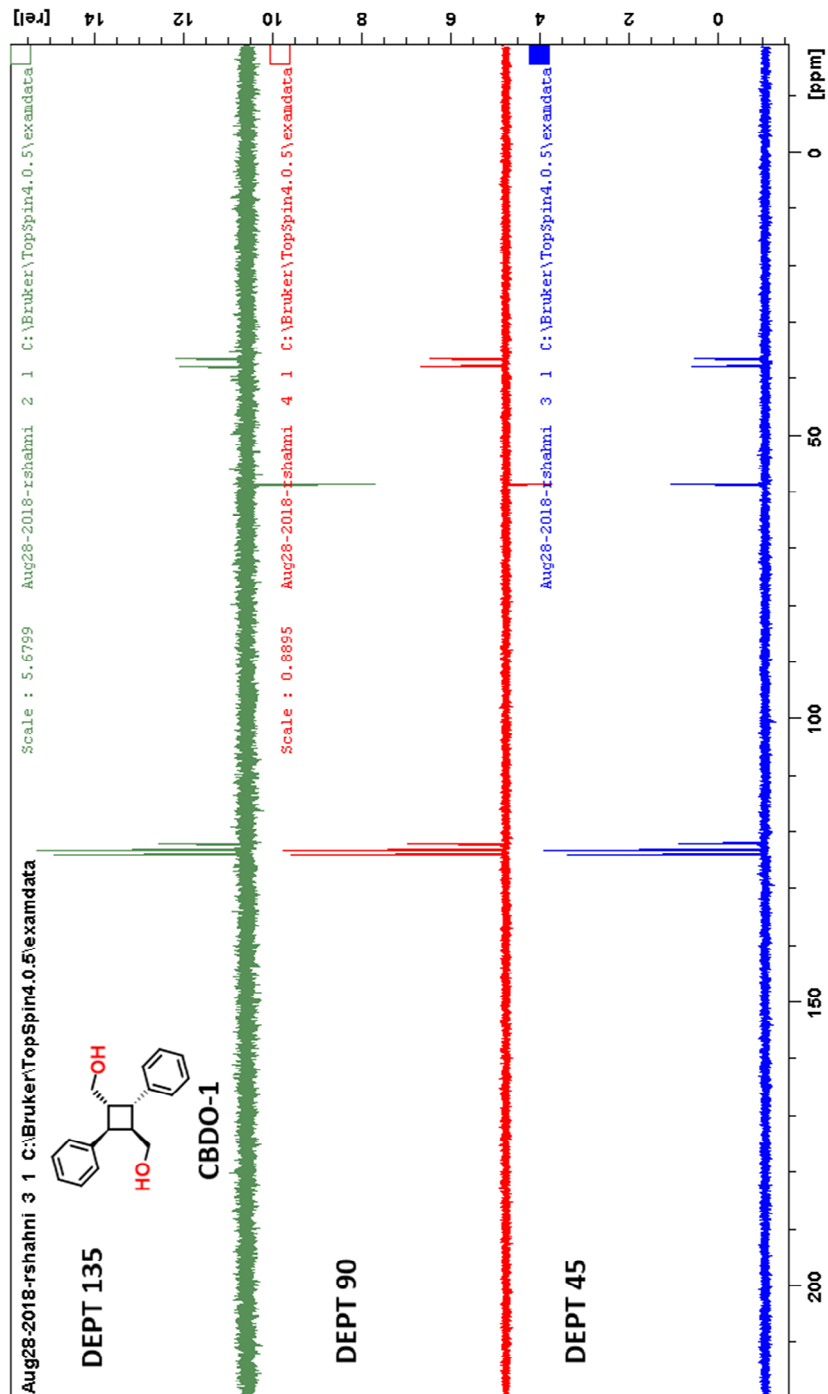


Figure S7. DEPT 45, 90 and 135 spectra of **CBDO-1** in CDCl_3 at room temperature.

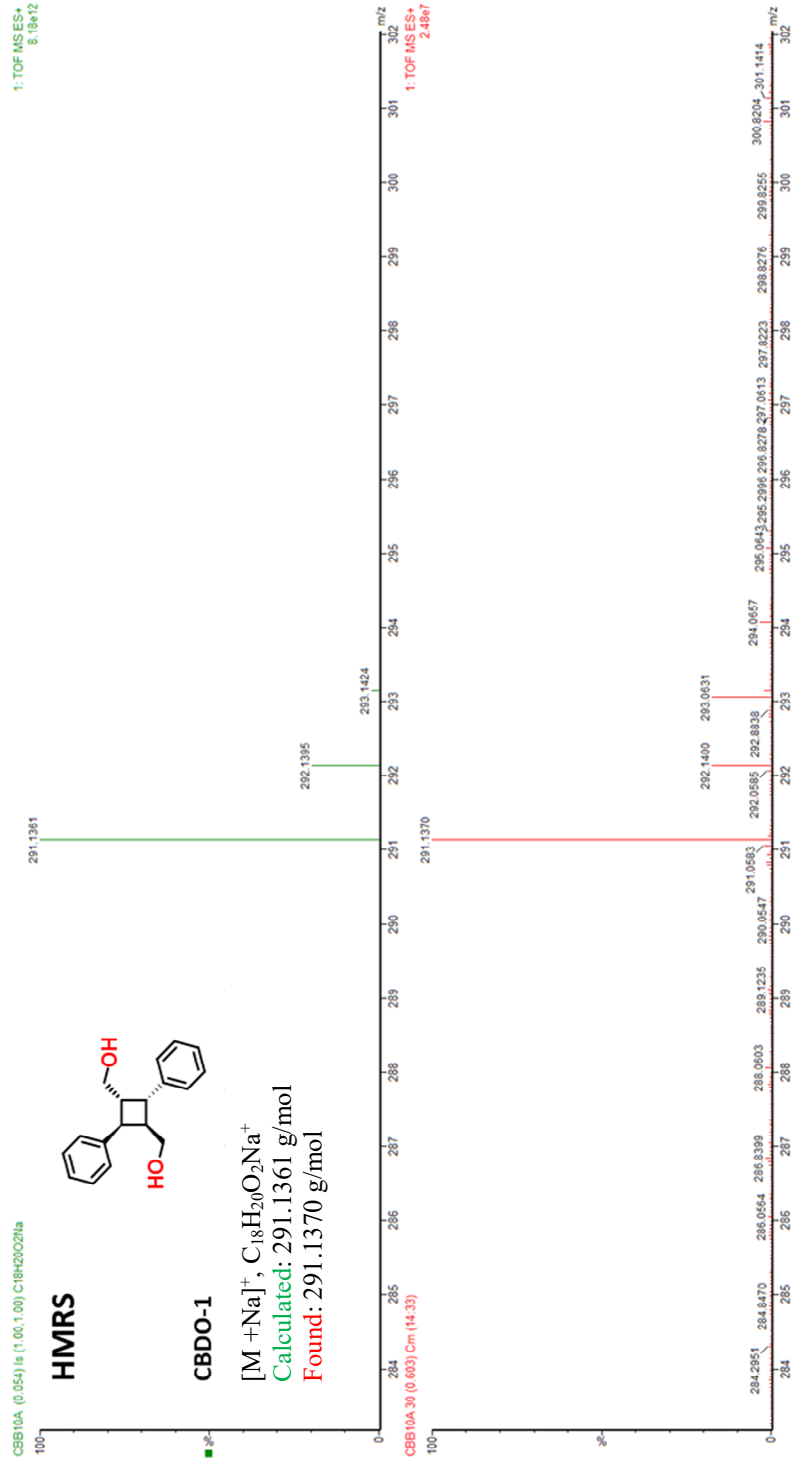


Figure S8. High resolution mass spectrometry of **CBDO-1**.

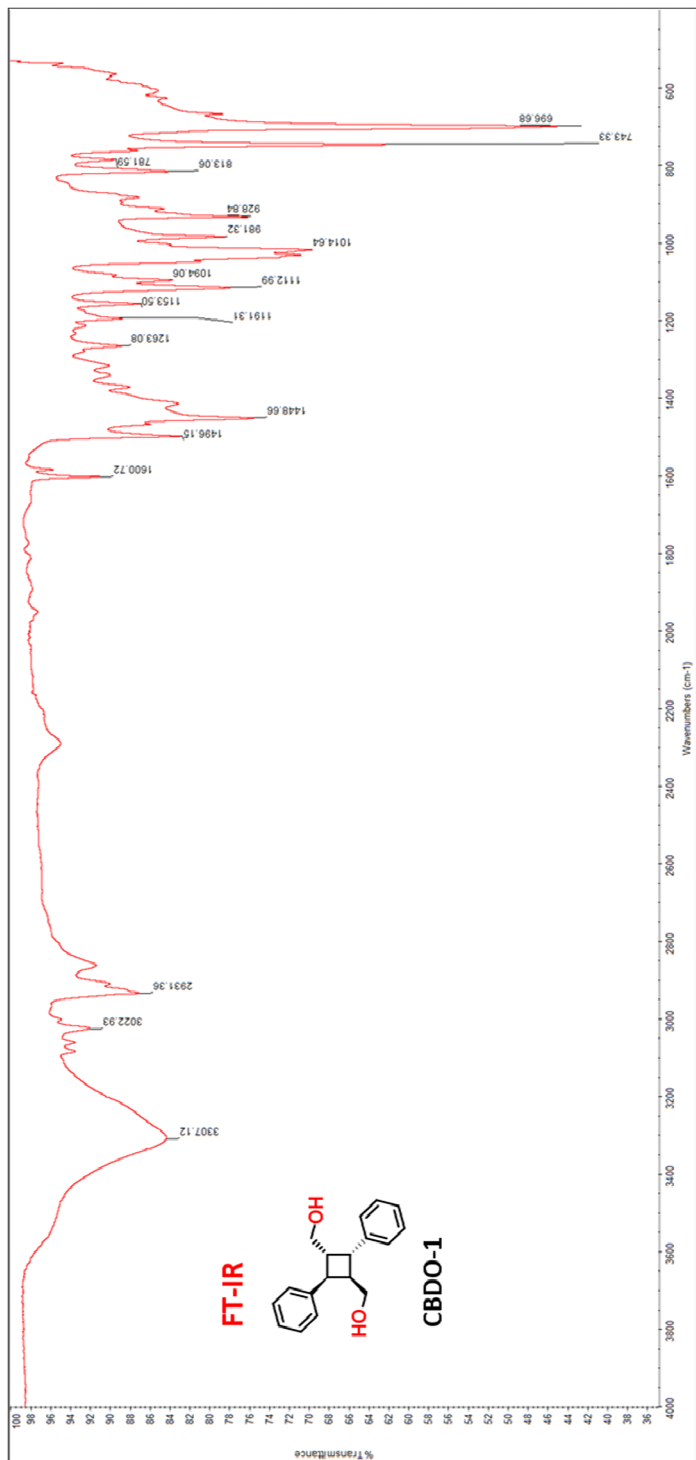


Figure S9. FT-IR spectrum of **CBDO-1** using ATR detector.

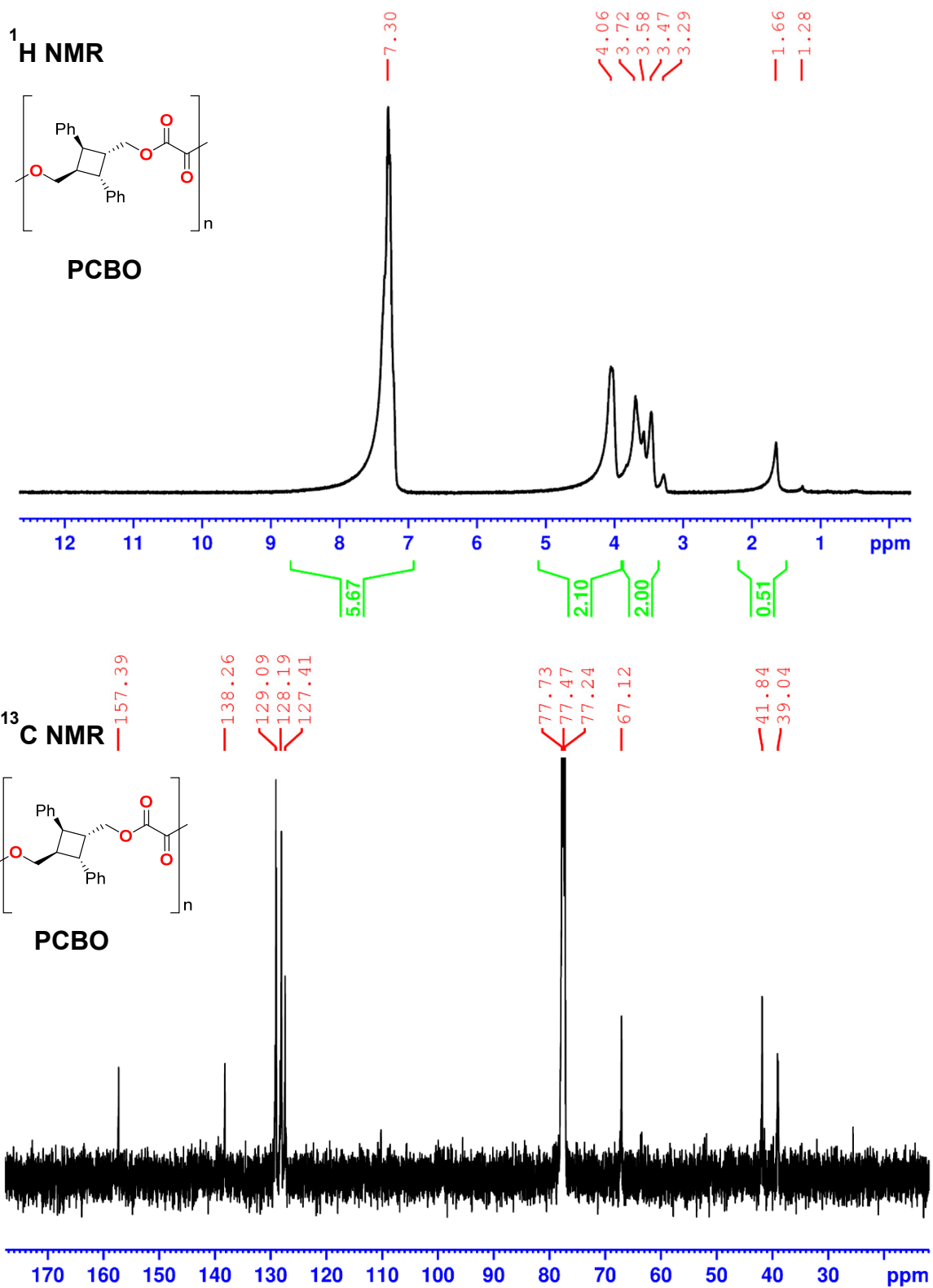


Figure S10. ^1H and ^{13}C NMR spectra of PCBO in CDCl_3 at room temperature

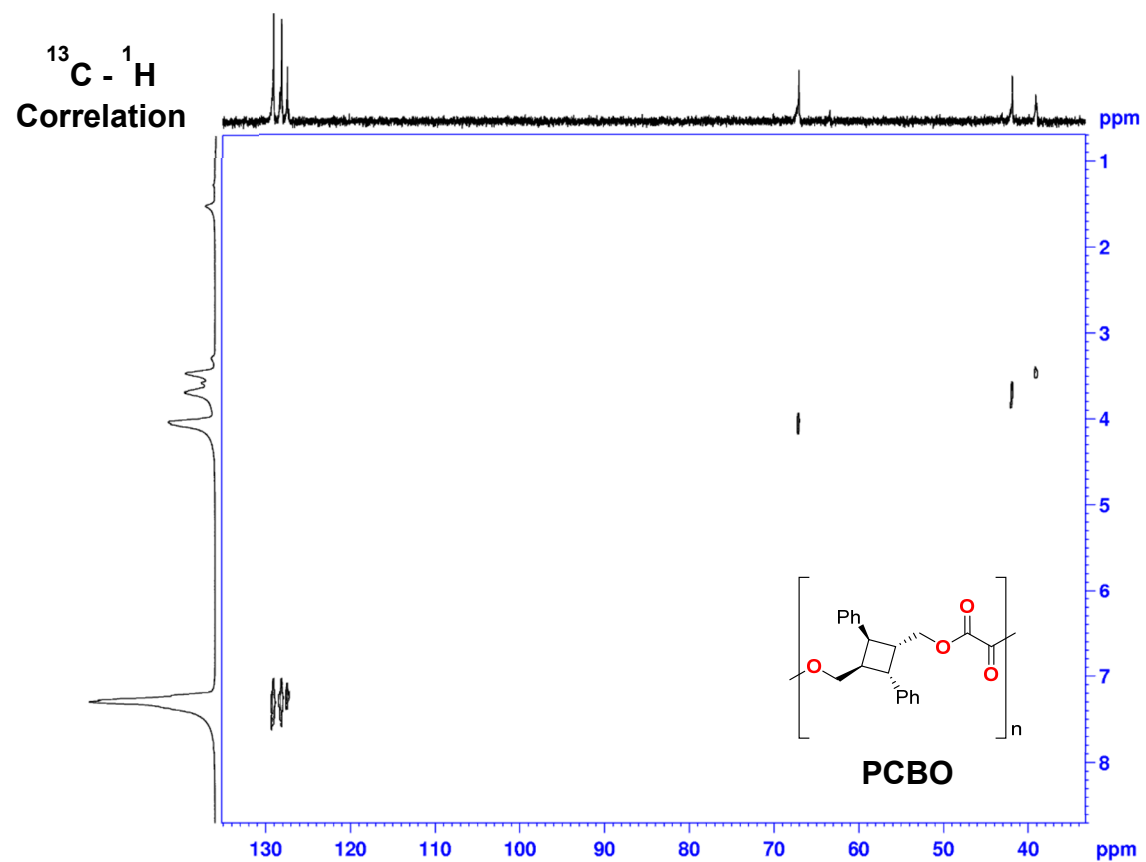
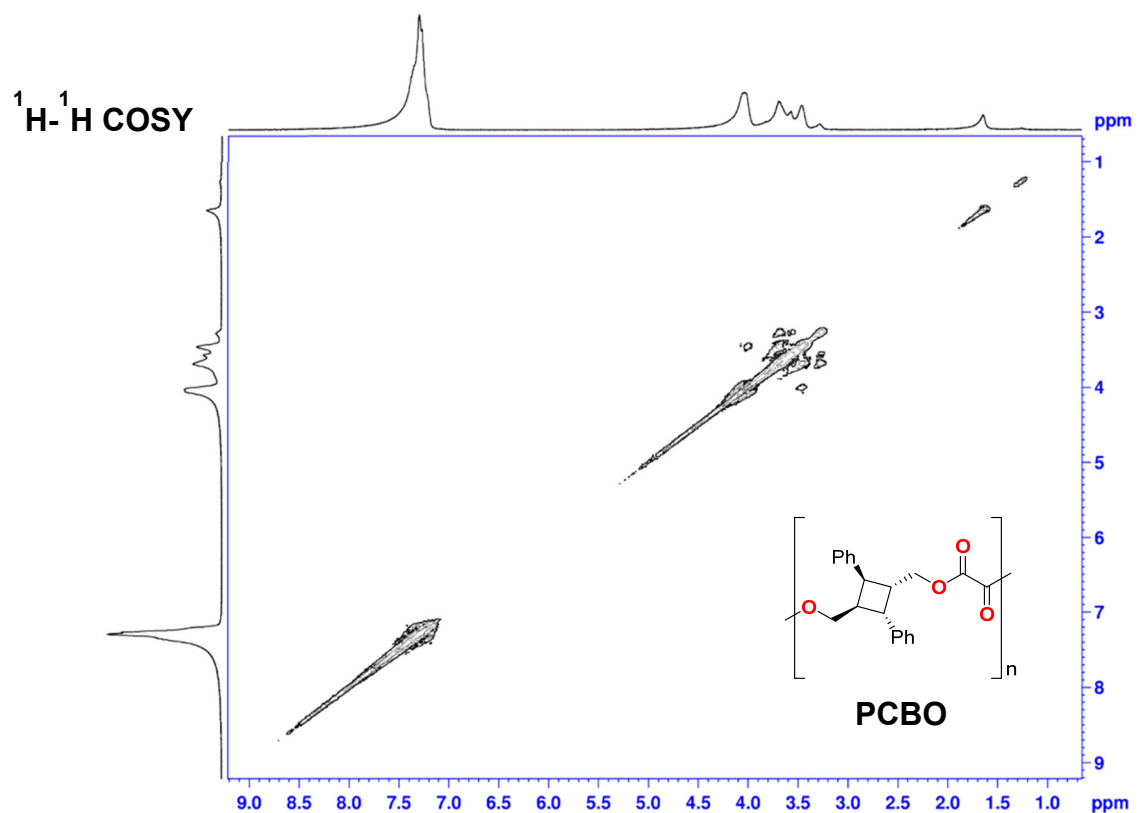


Figure S11. COSY and CH-correlation spectra of **PCBO** in CDCl_3 at room temperature.

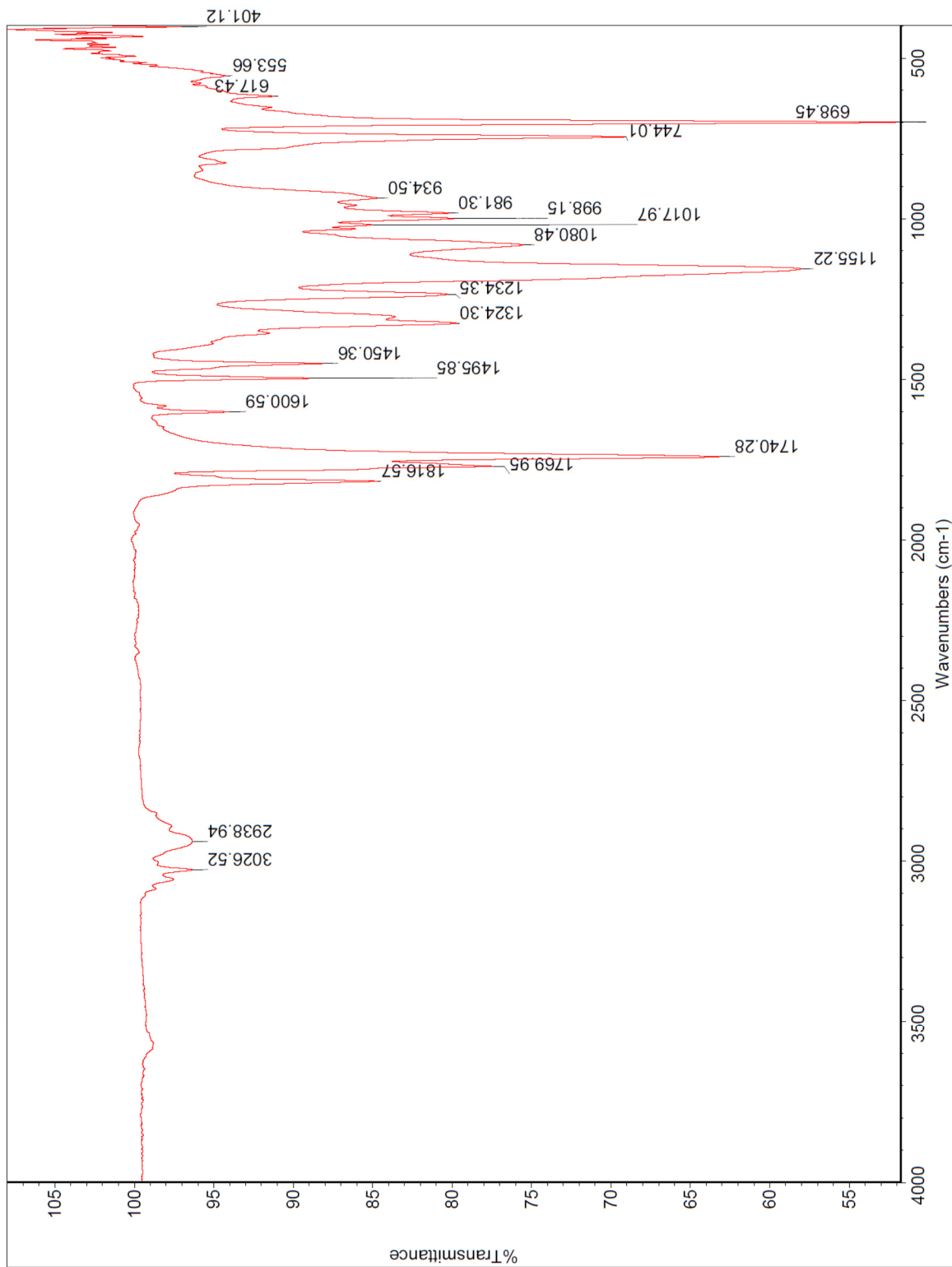


Figure S12. FT-IR spectrum of **PCBO** using ATR detector.

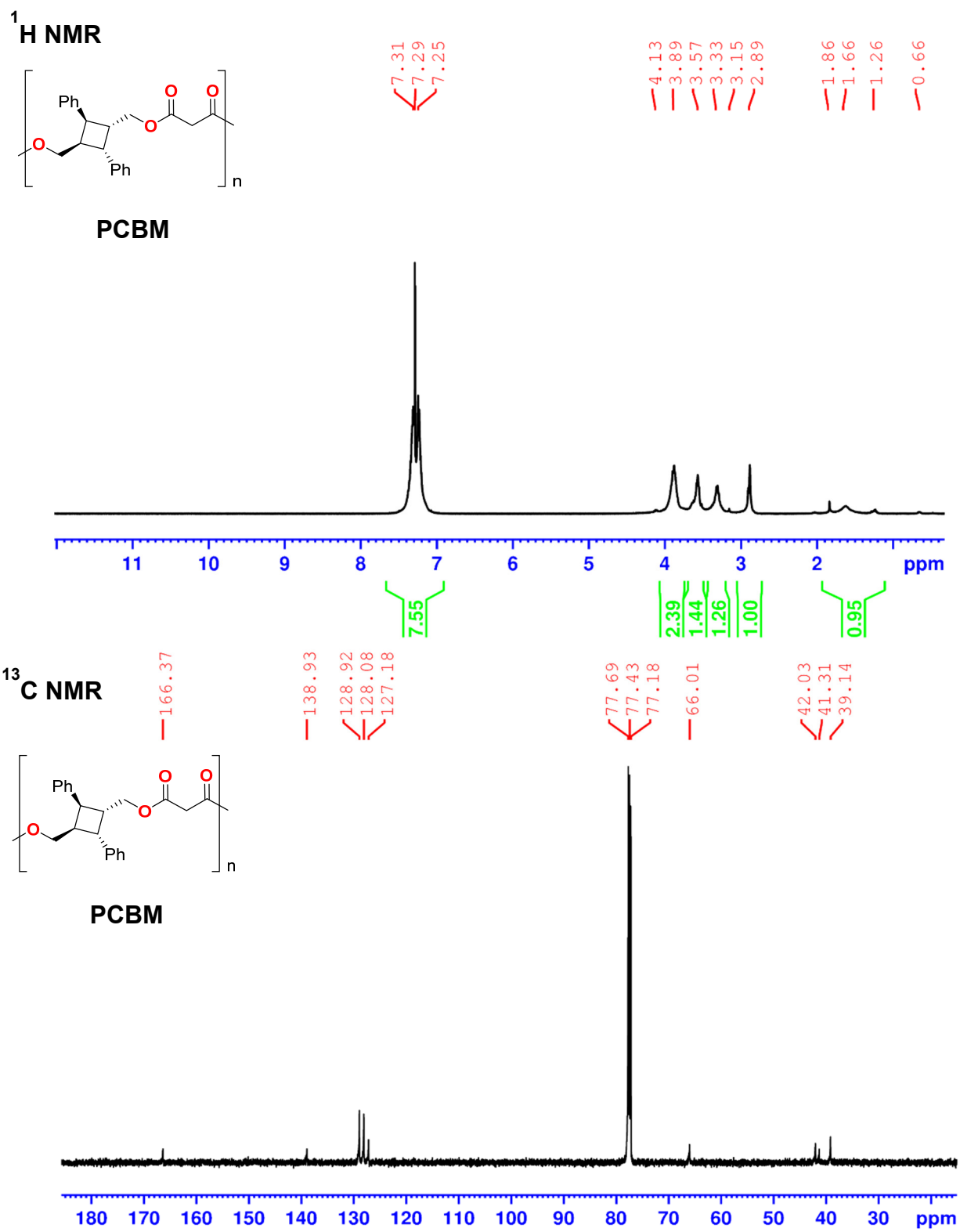


Figure S13. ¹H and ¹³C NMR spectra of **PCBM** in CDCl₃ at room temperature.

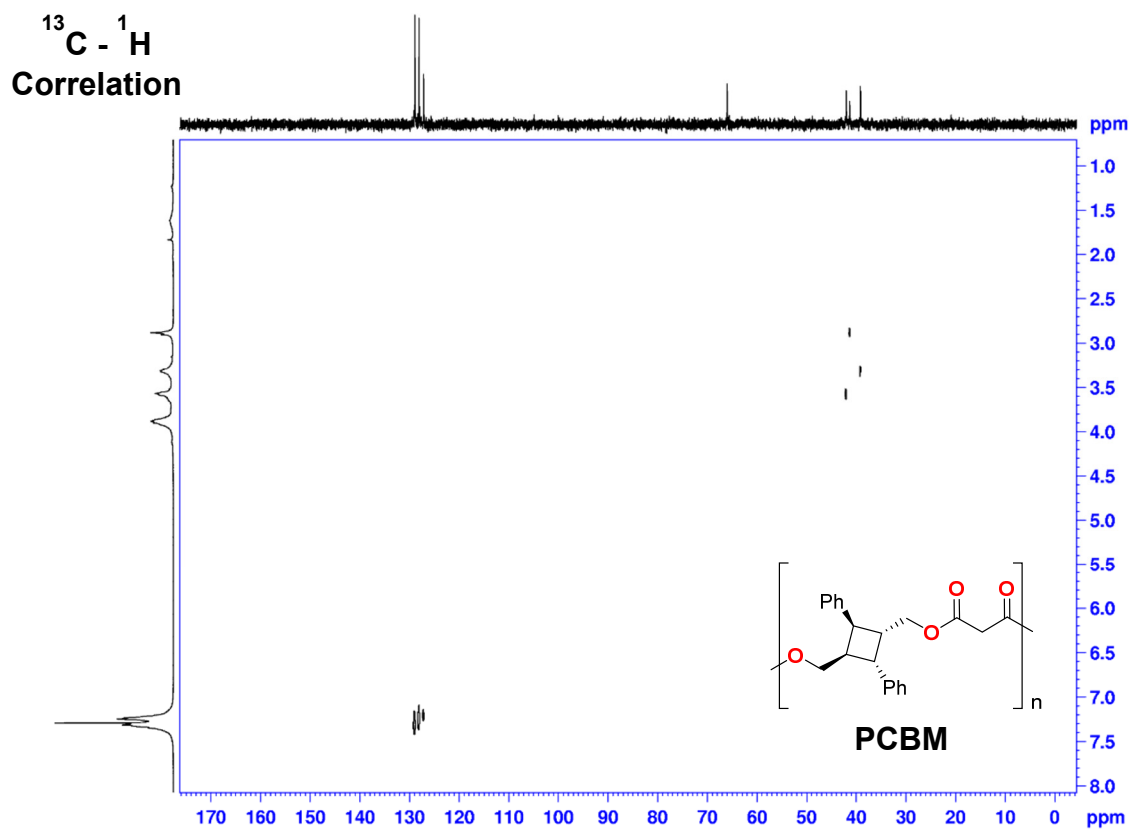
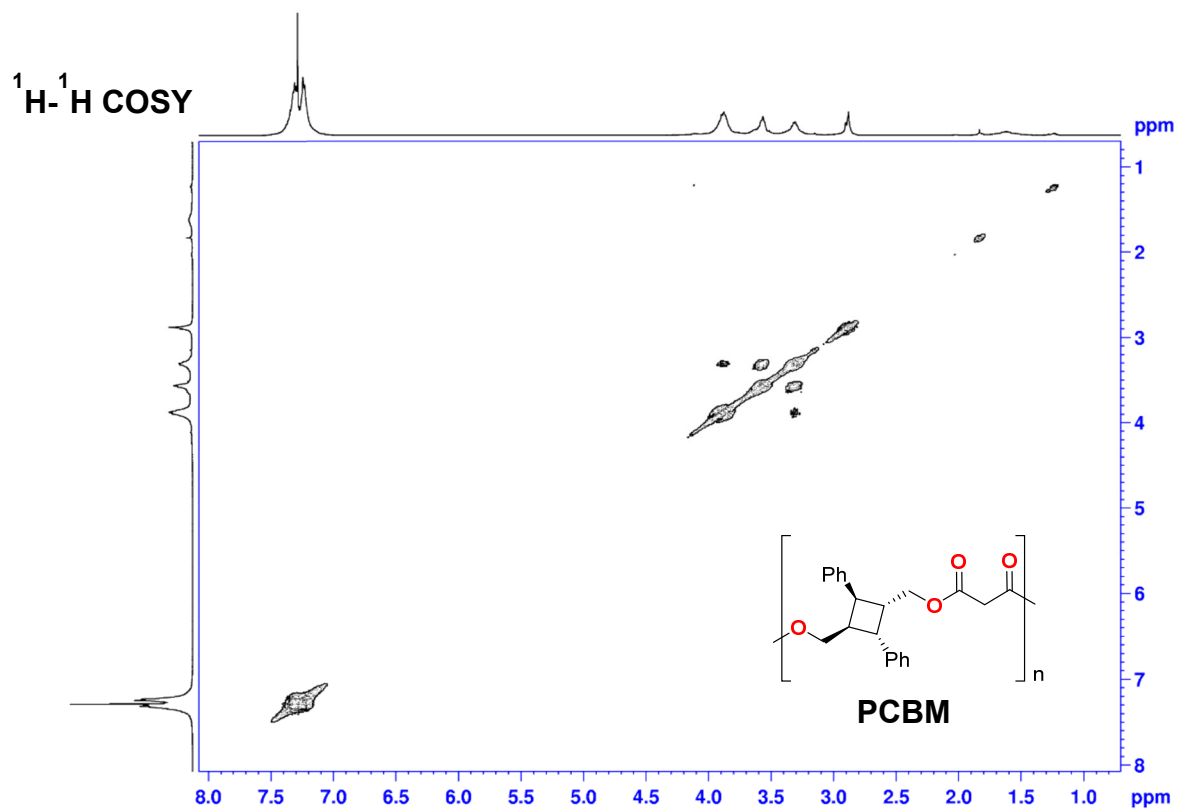


Figure S14.COSY and C-H correlation spectra of PCBM in CDCl_3 at room temperature.

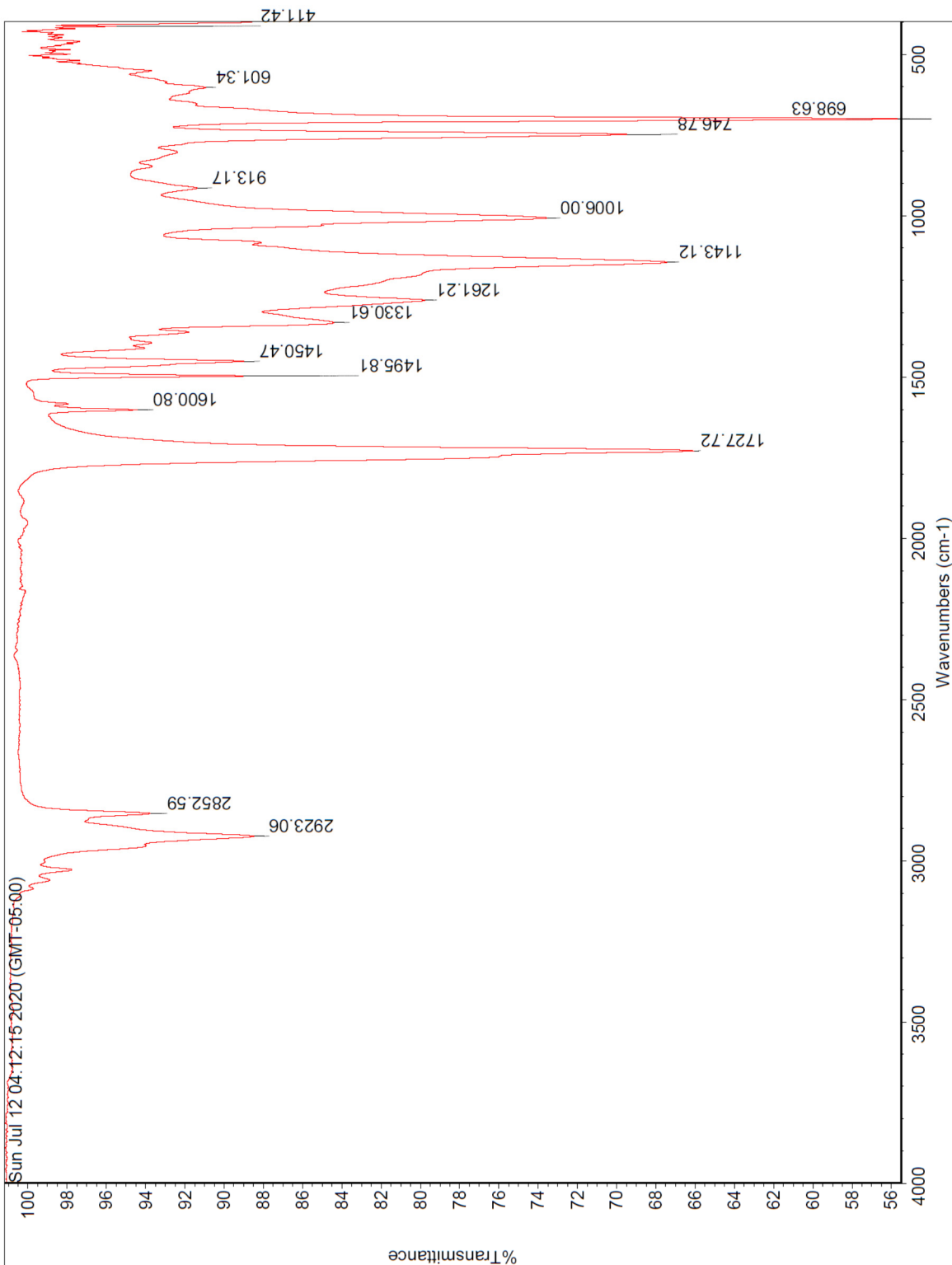
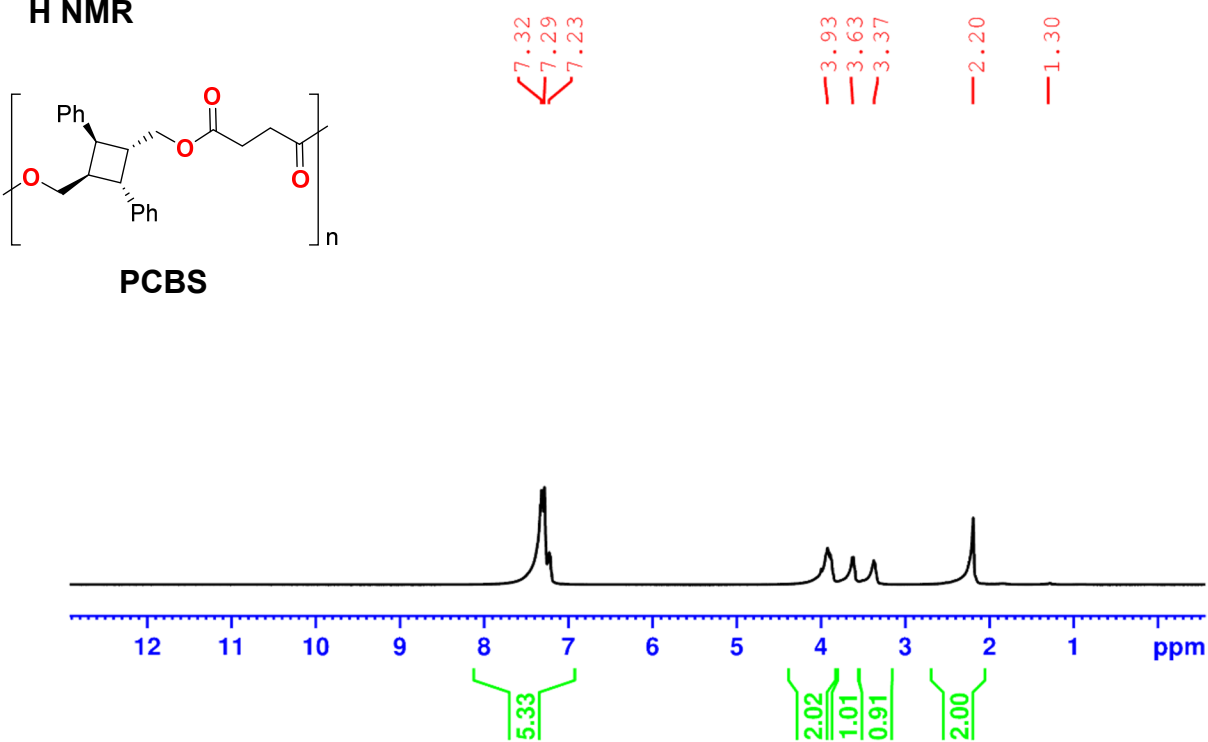


Figure S15. FT-IR spectrum of **PCBM** using ATR detector.

¹H NMR



¹³C NMR

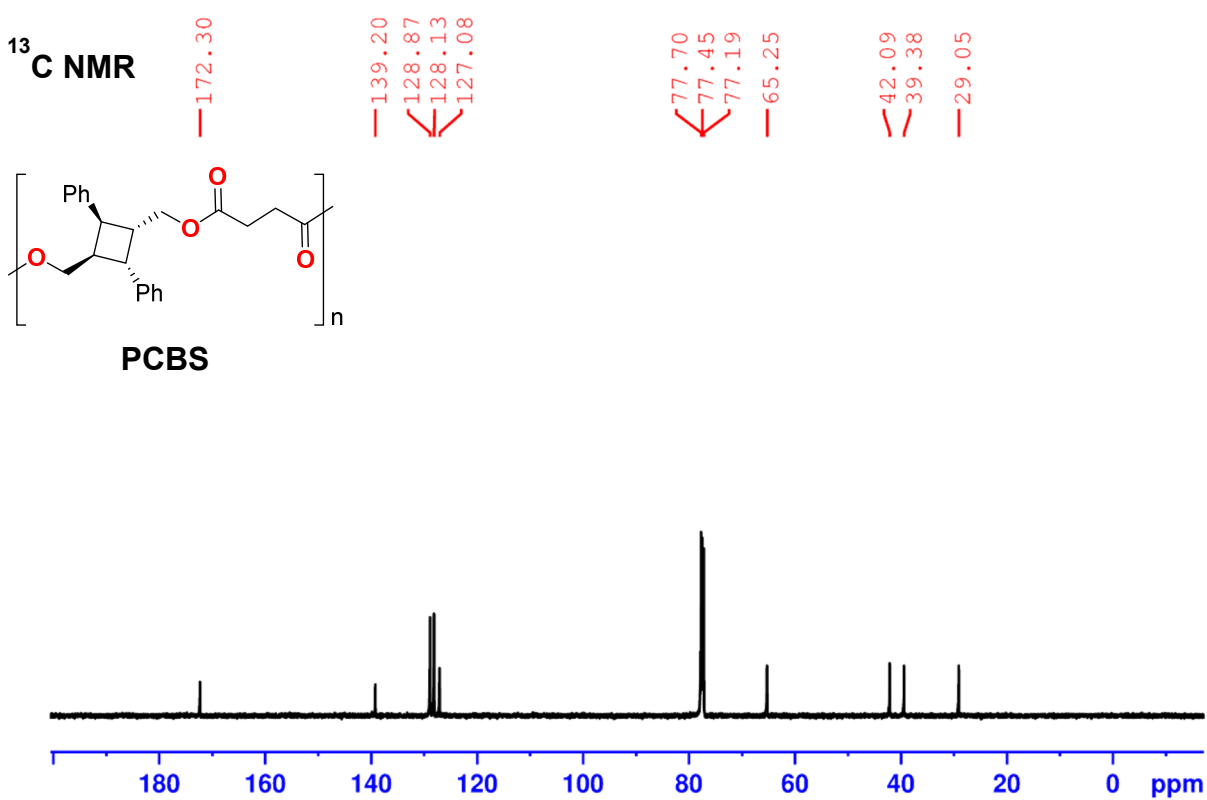


Figure S16. ¹H and ¹³C NMR spectra of PCBS in CDCl₃ at room temperature.

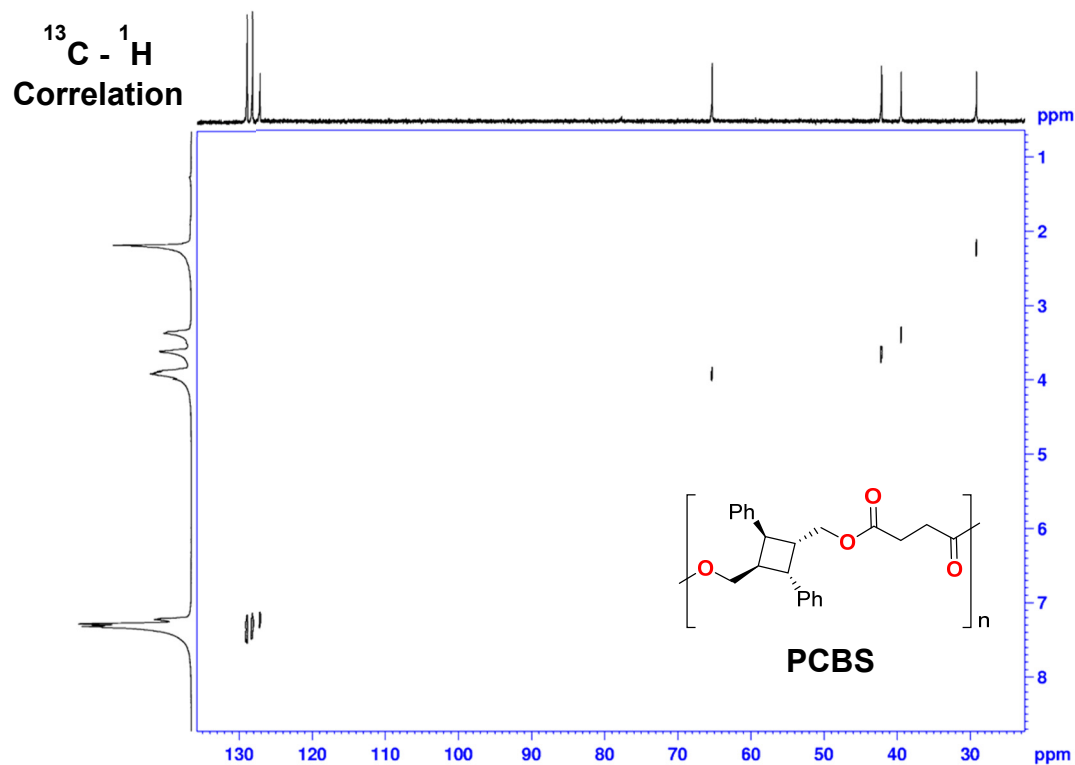
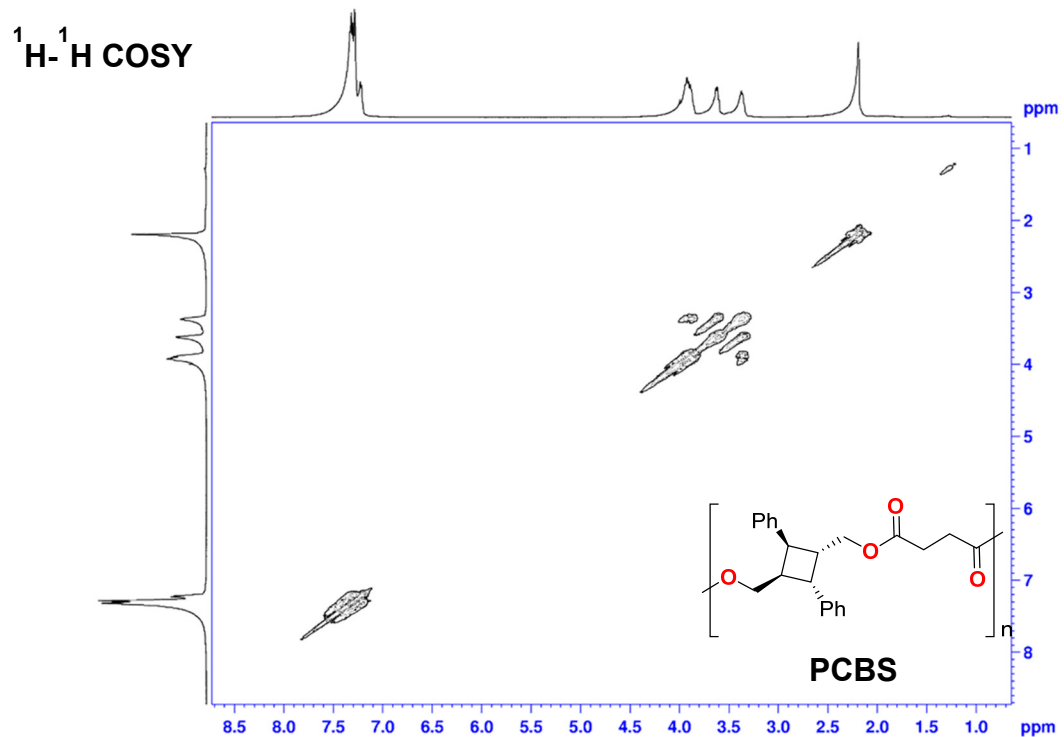


Figure S17.COSY and C-H correlation spectra of PCBS in CDCl_3 at room temperature.

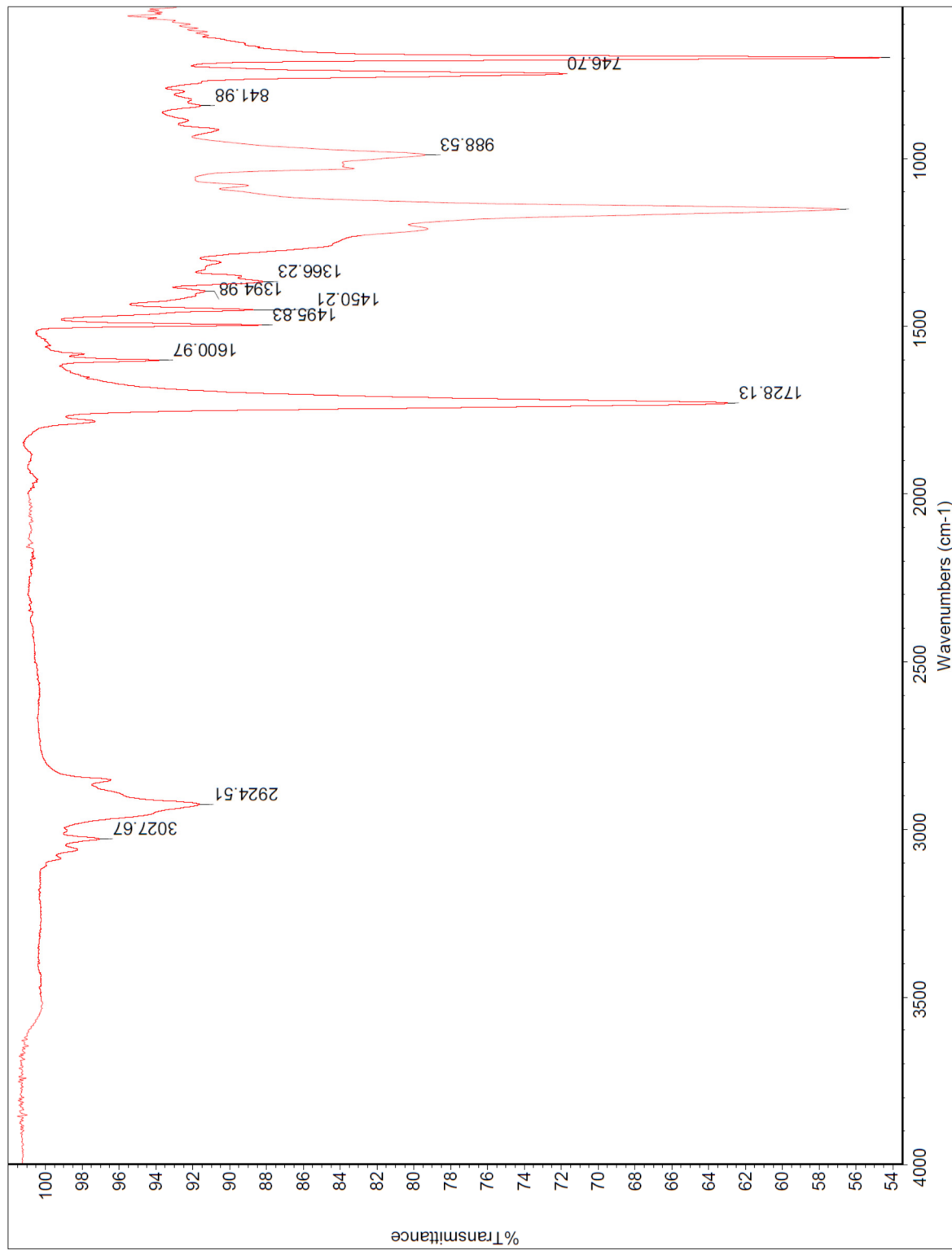
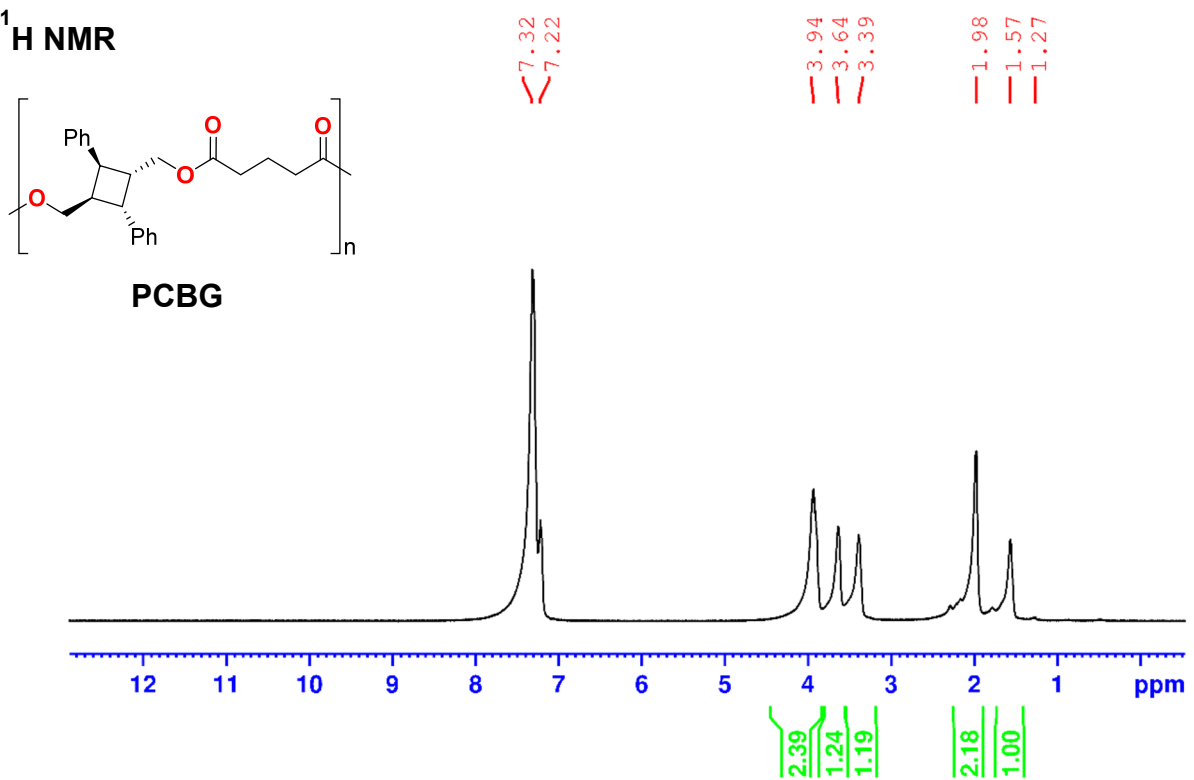


Figure S18. FT-IR spectrum of **PCBS** using ATR detector.

¹H NMR



¹³C NMR

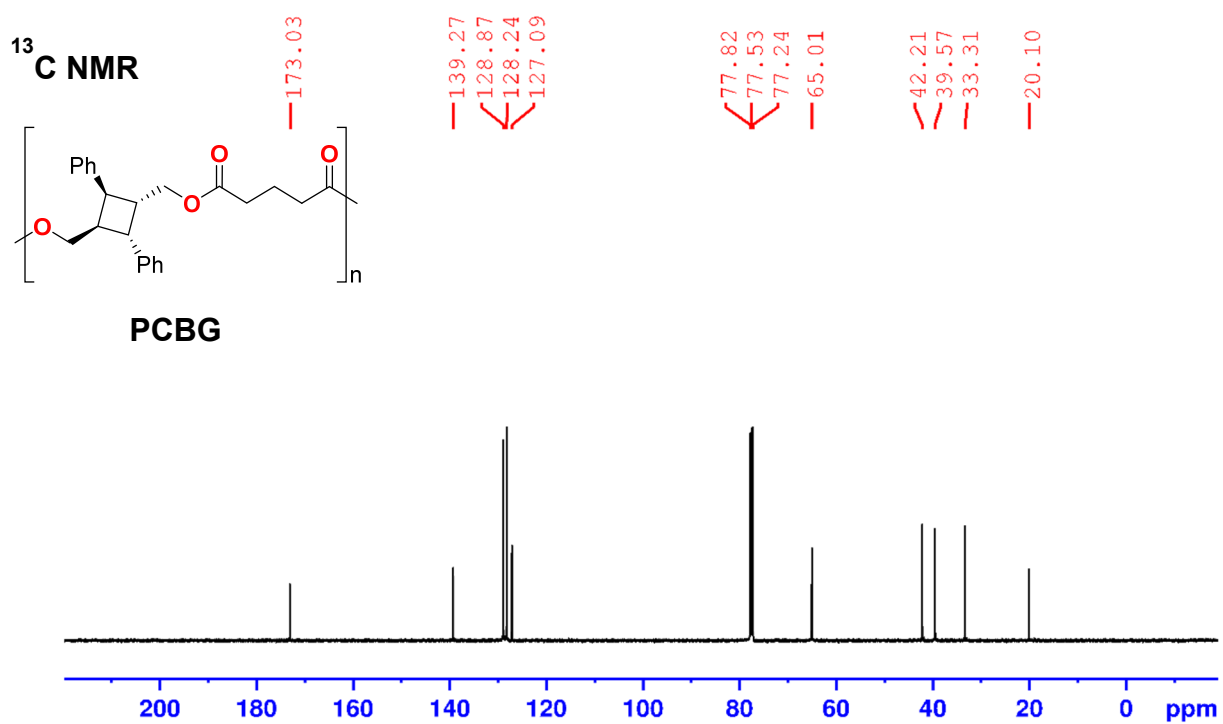


Figure S19. ¹H and ¹³C NMR spectra of PCBG in CDCl₃ at room temperature.

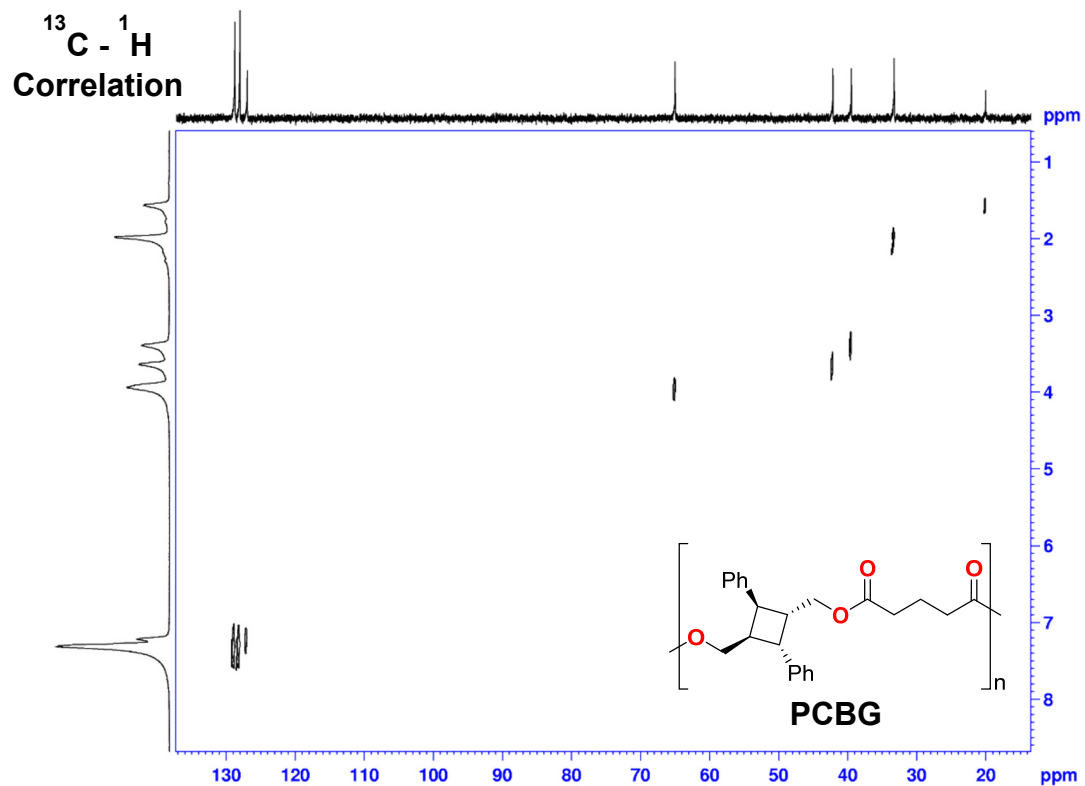
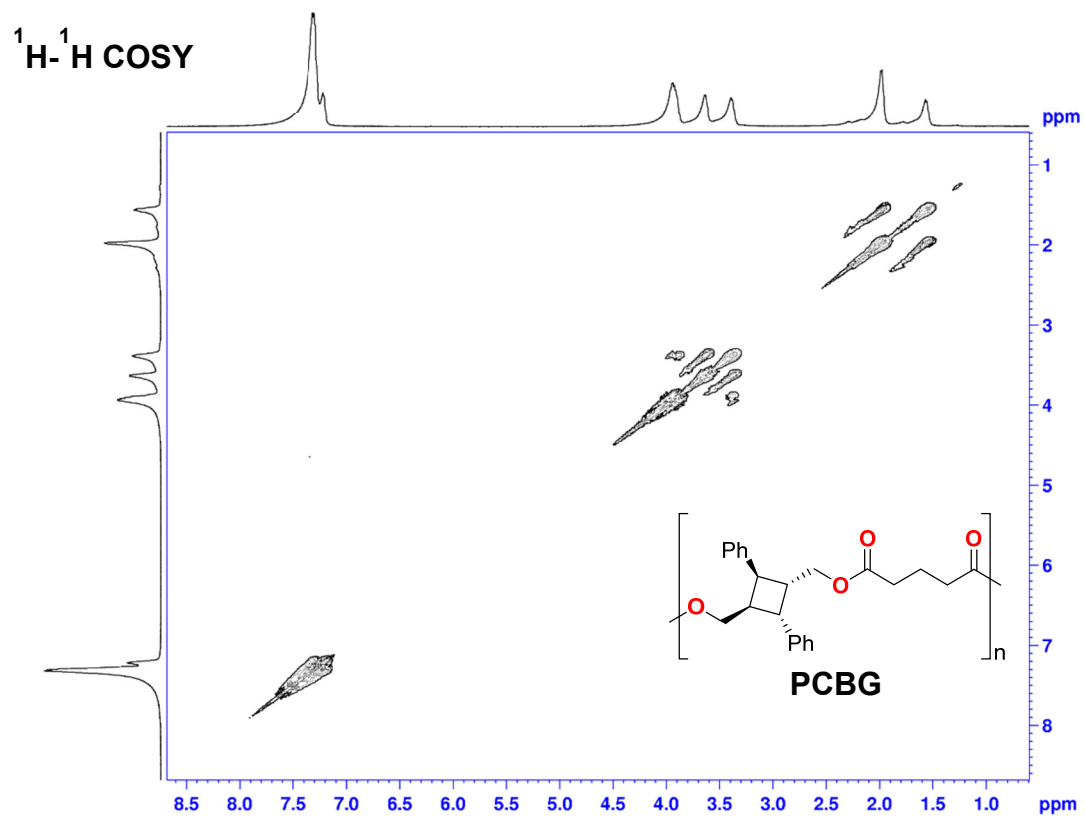


Figure S20.COSY and C-H correlation spectra of PCBG in CDCl₃ at room temperature.

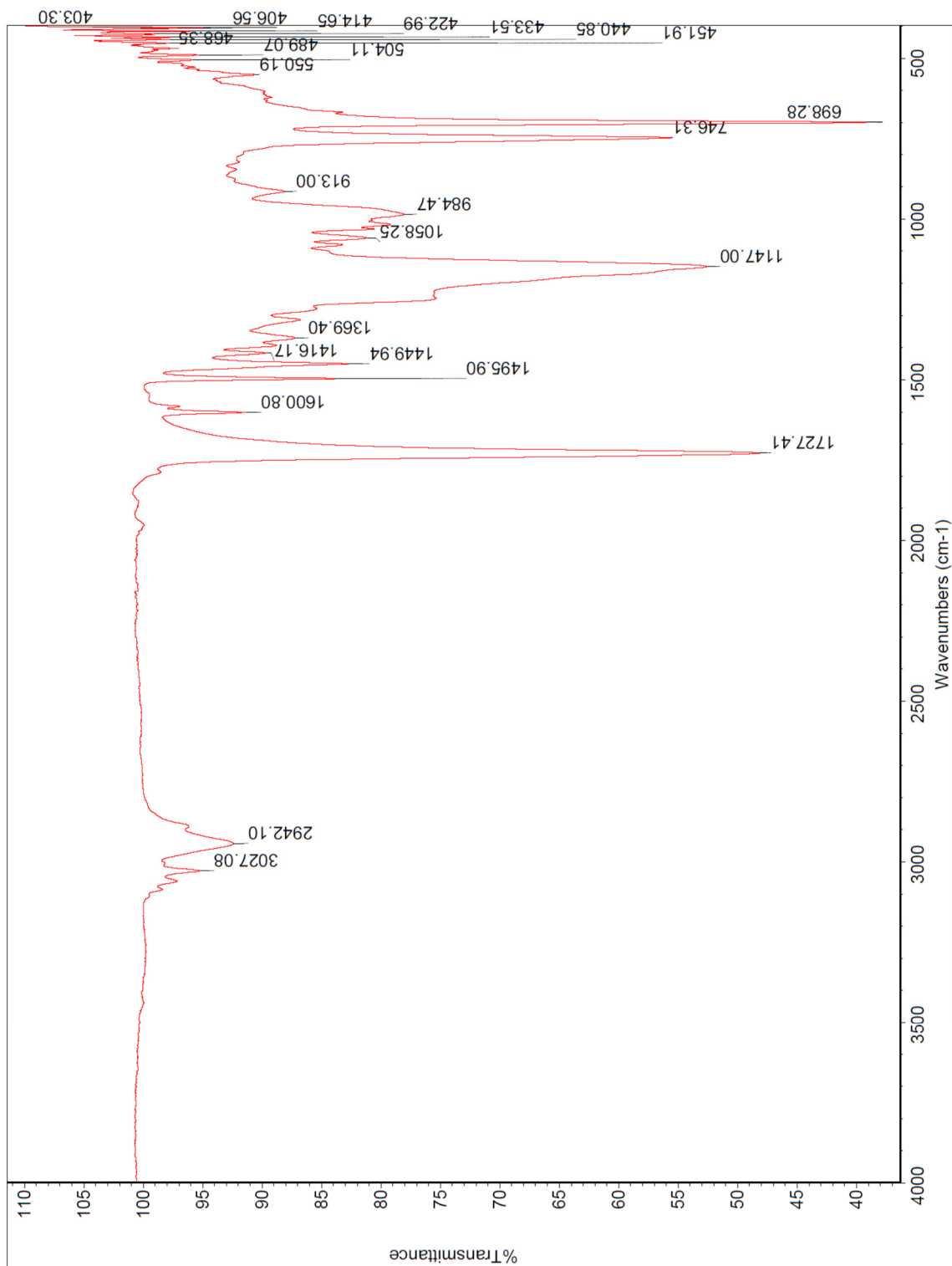


Figure S21. FT-IR spectrum of **PCBG** using ATR detector

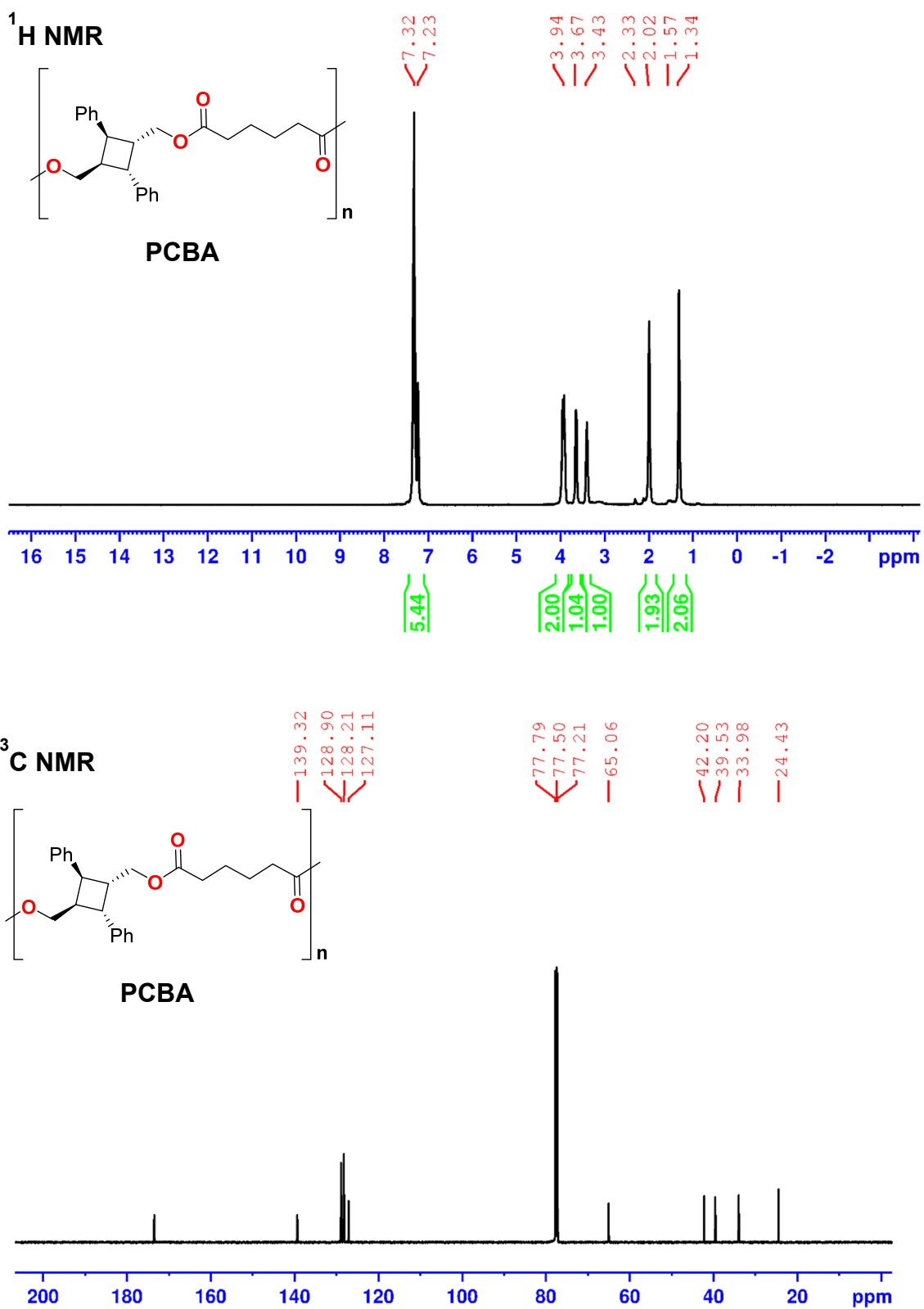


Figure S22. ^1H and ^{13}C NMR spectra of PCBA in CDCl_3 at room temperature.

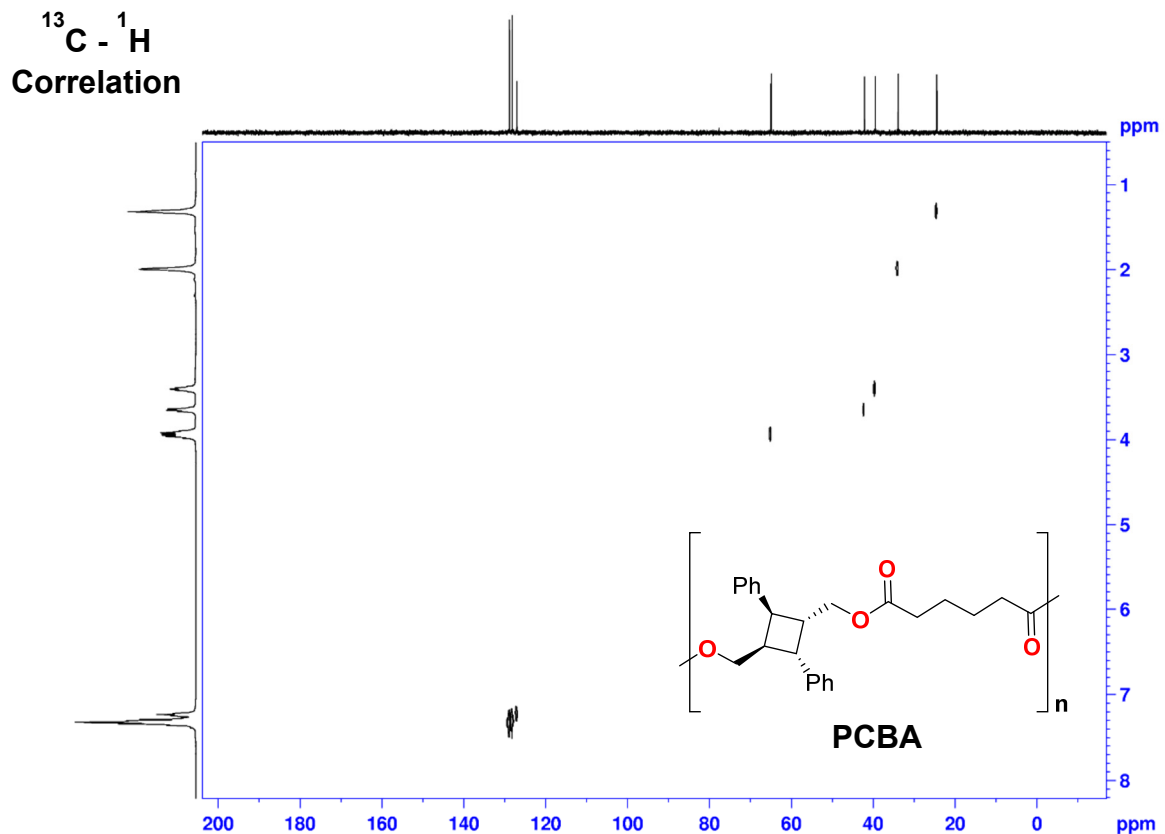
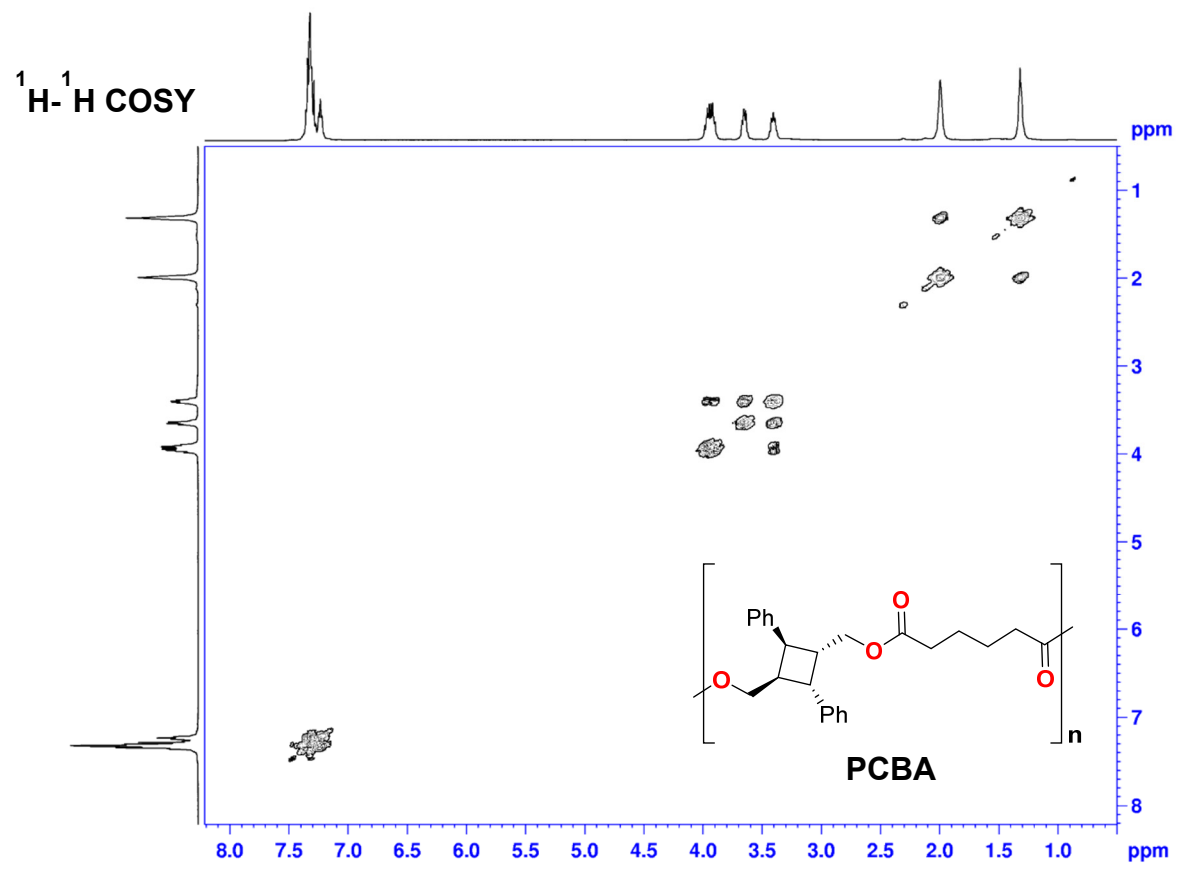


Figure S23.COSY and C-H correlation spectra of PCBA in CDCl_3 at room temperature.

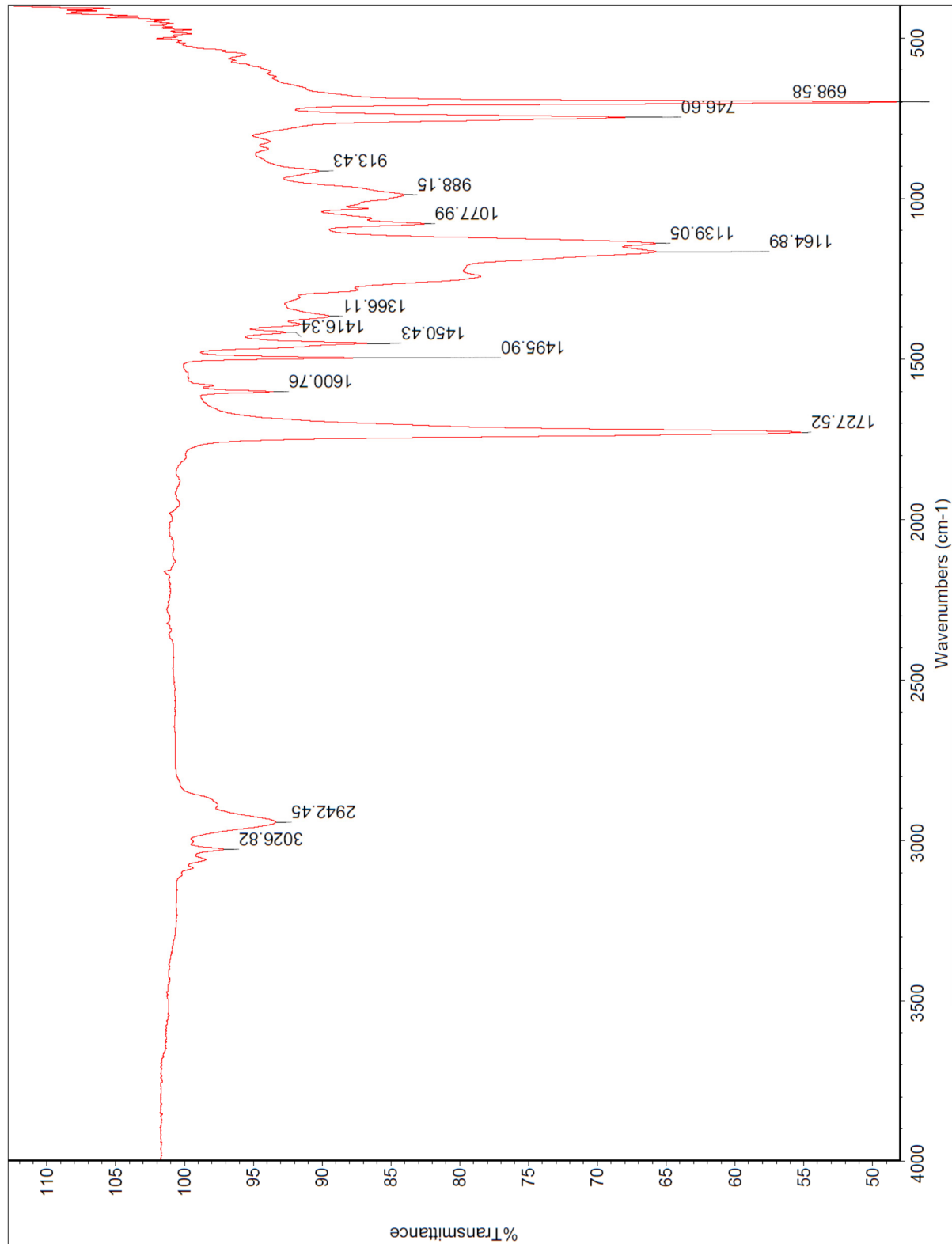


Figure S24. FT-IR spectrum of PCBA using ATR detector.

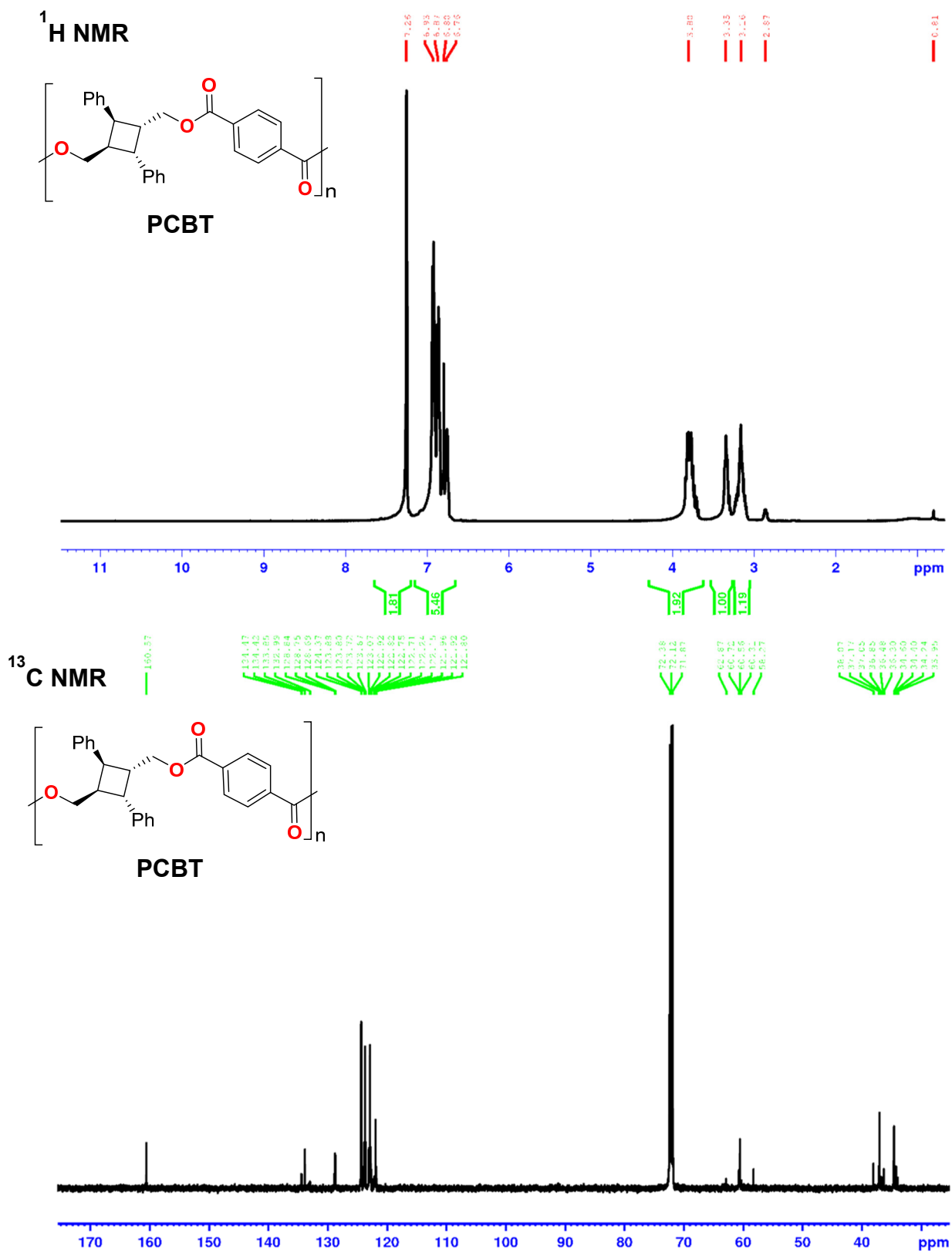


Figure S25. ^1H and ^{13}C NMR spectra of PCBT in CDCl_3 at room temperature.

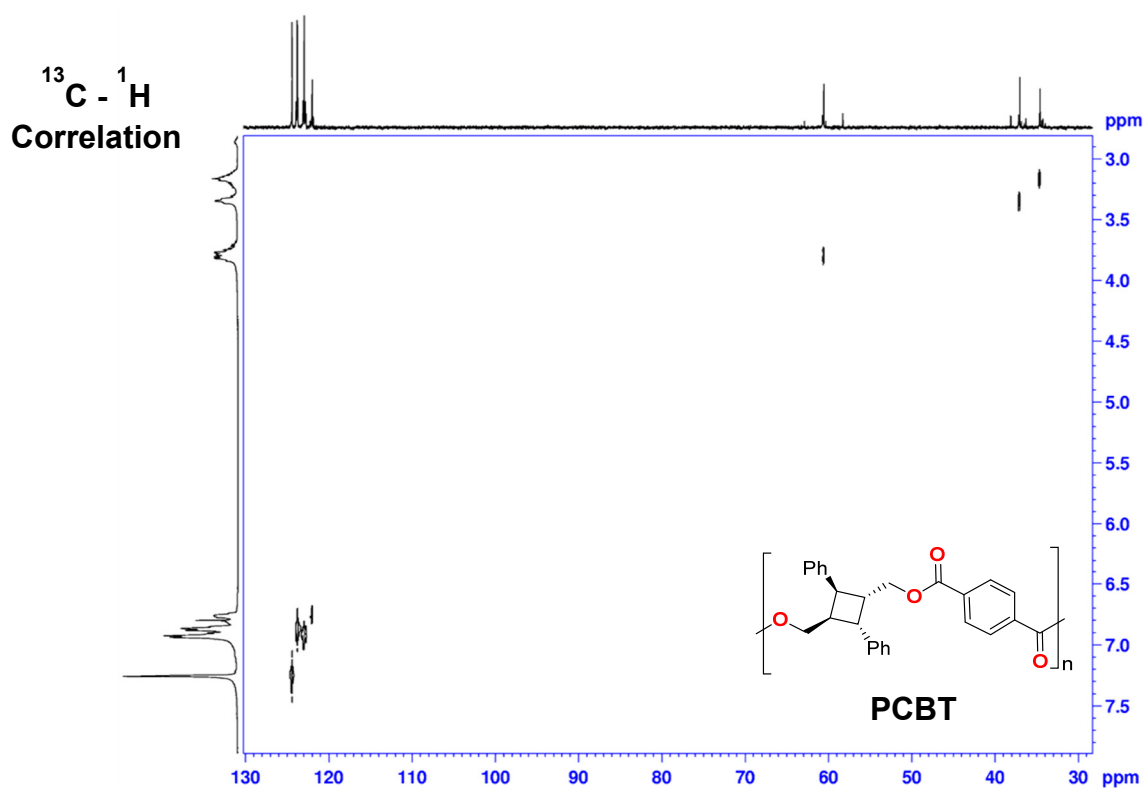
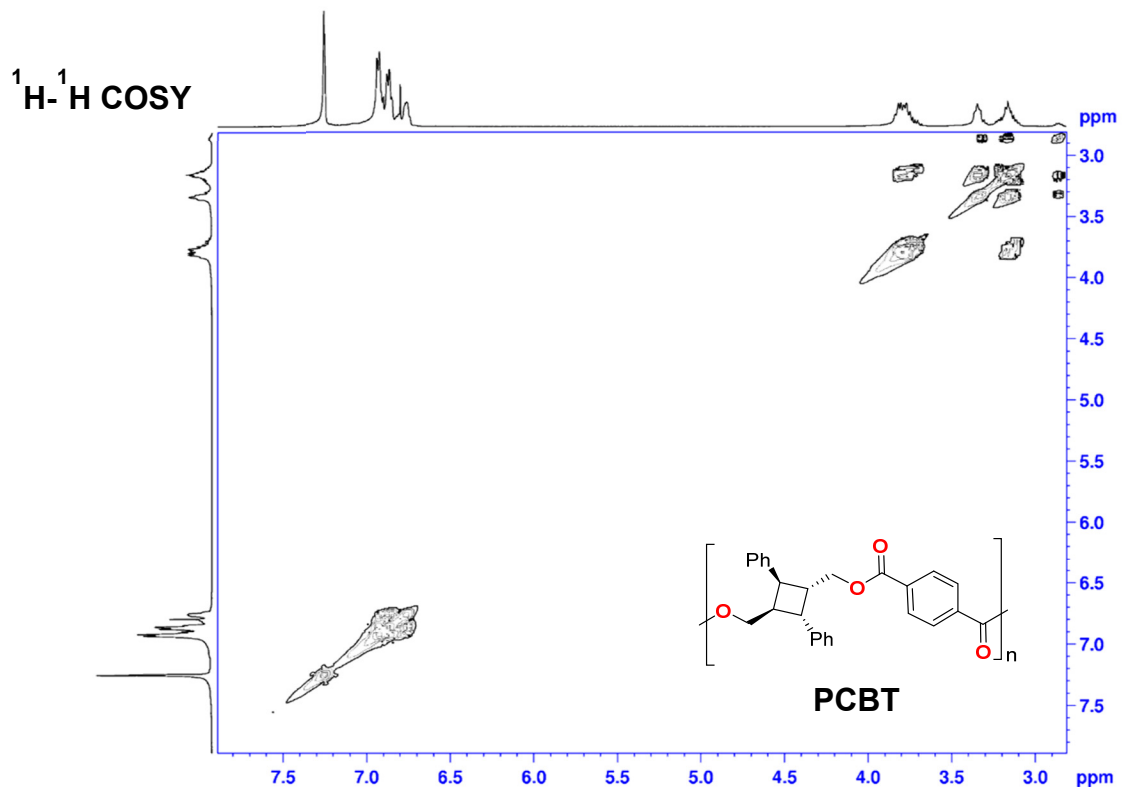


Figure S26.COSY and C-H correlation spectra of PCBT in CDCl_3 at room temperature.

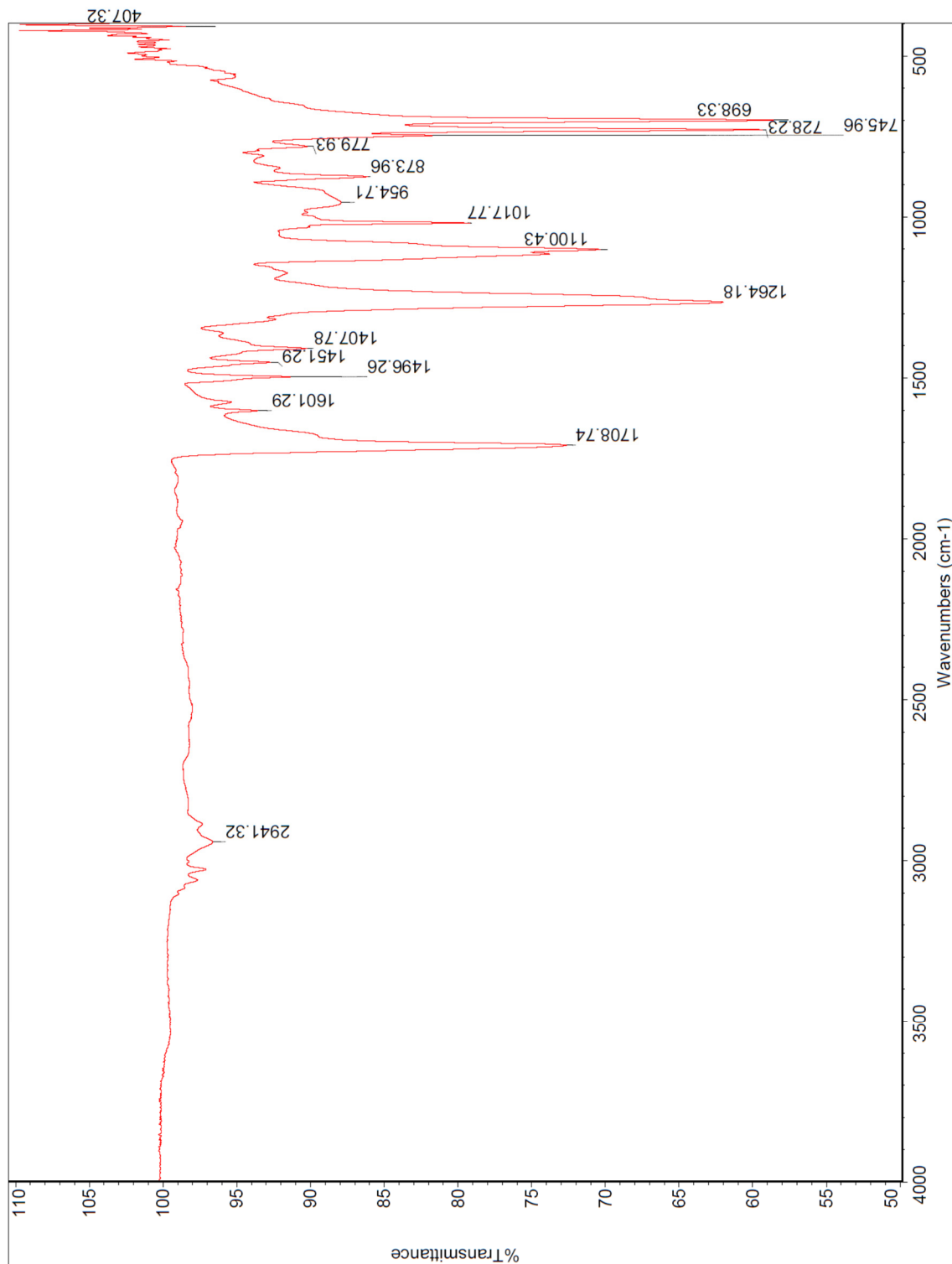


Figure S27. FT-IR of spectrum **PCBT** using ATR detector.

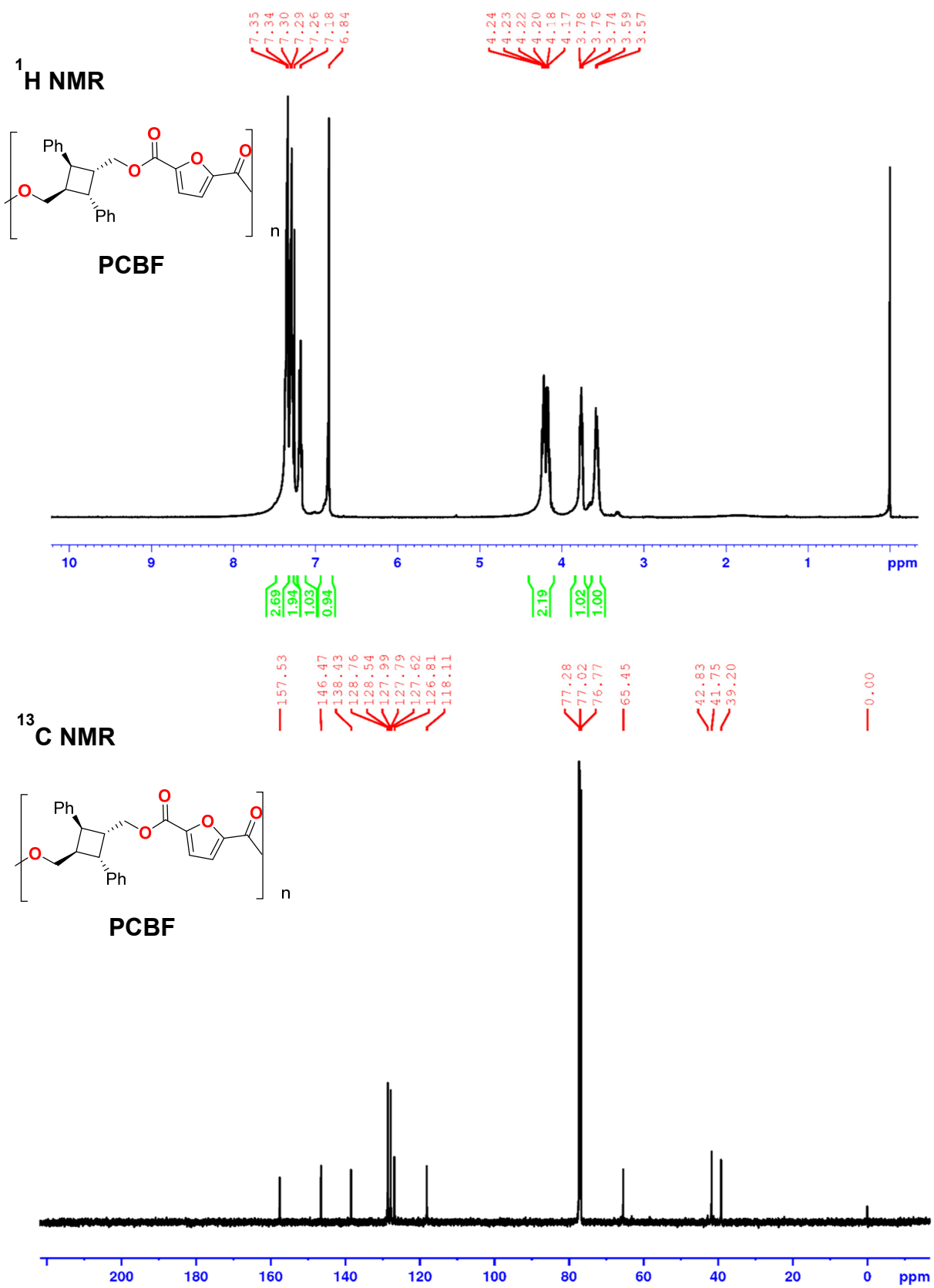


Figure S28. ^1H and ^{13}C NMR spectra of PCBF in CDCl_3 at room temperature.

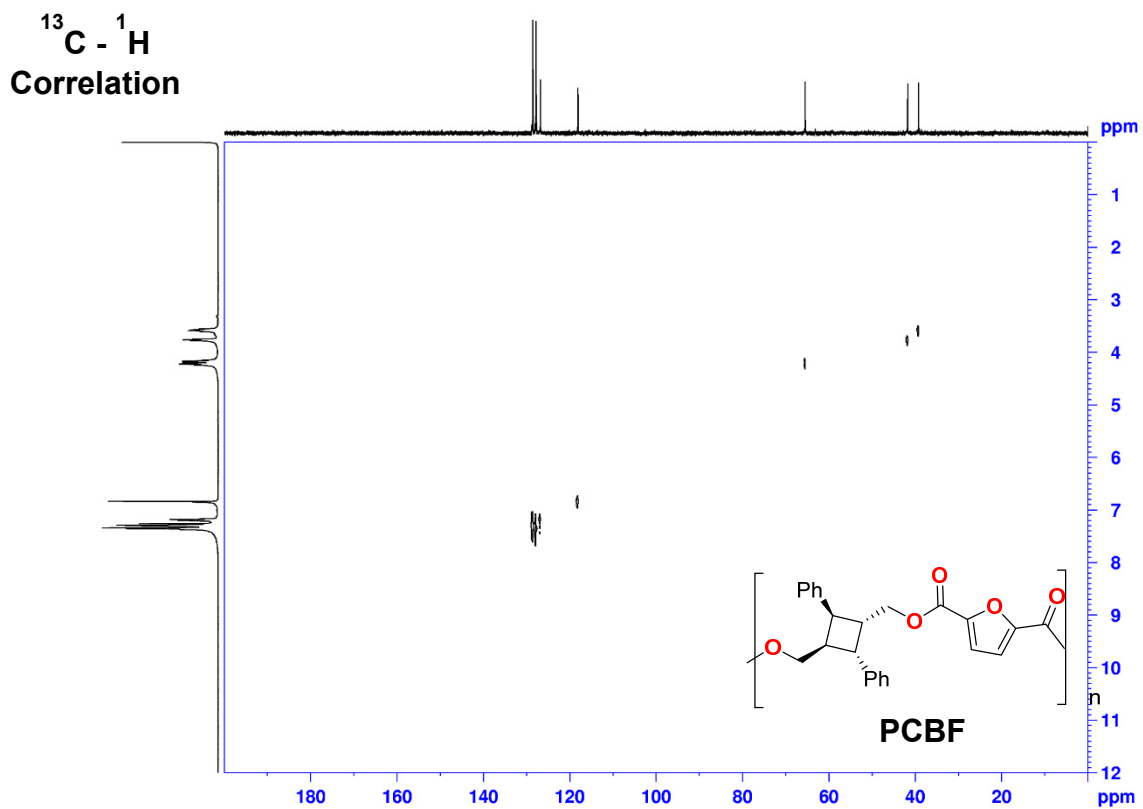
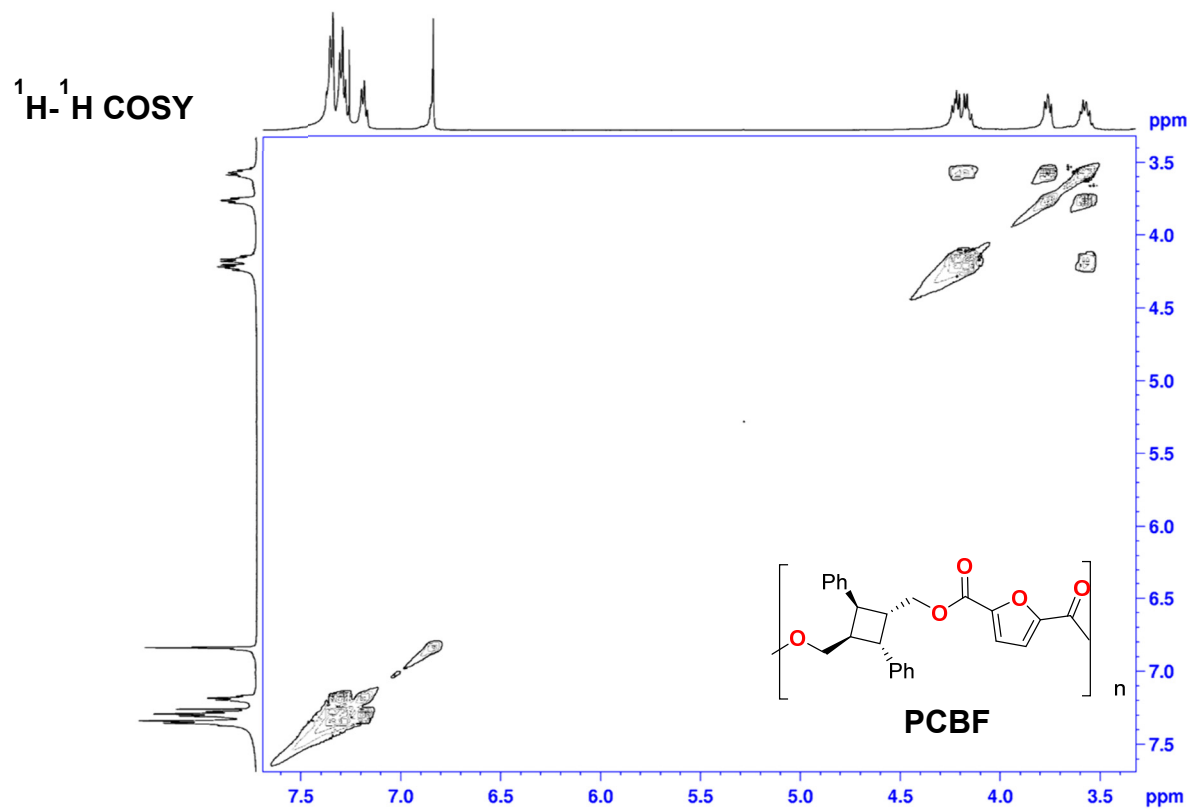


Figure S29.COSY and C-H correlation spectra of PCBF in CDCl_3 at room temperature.

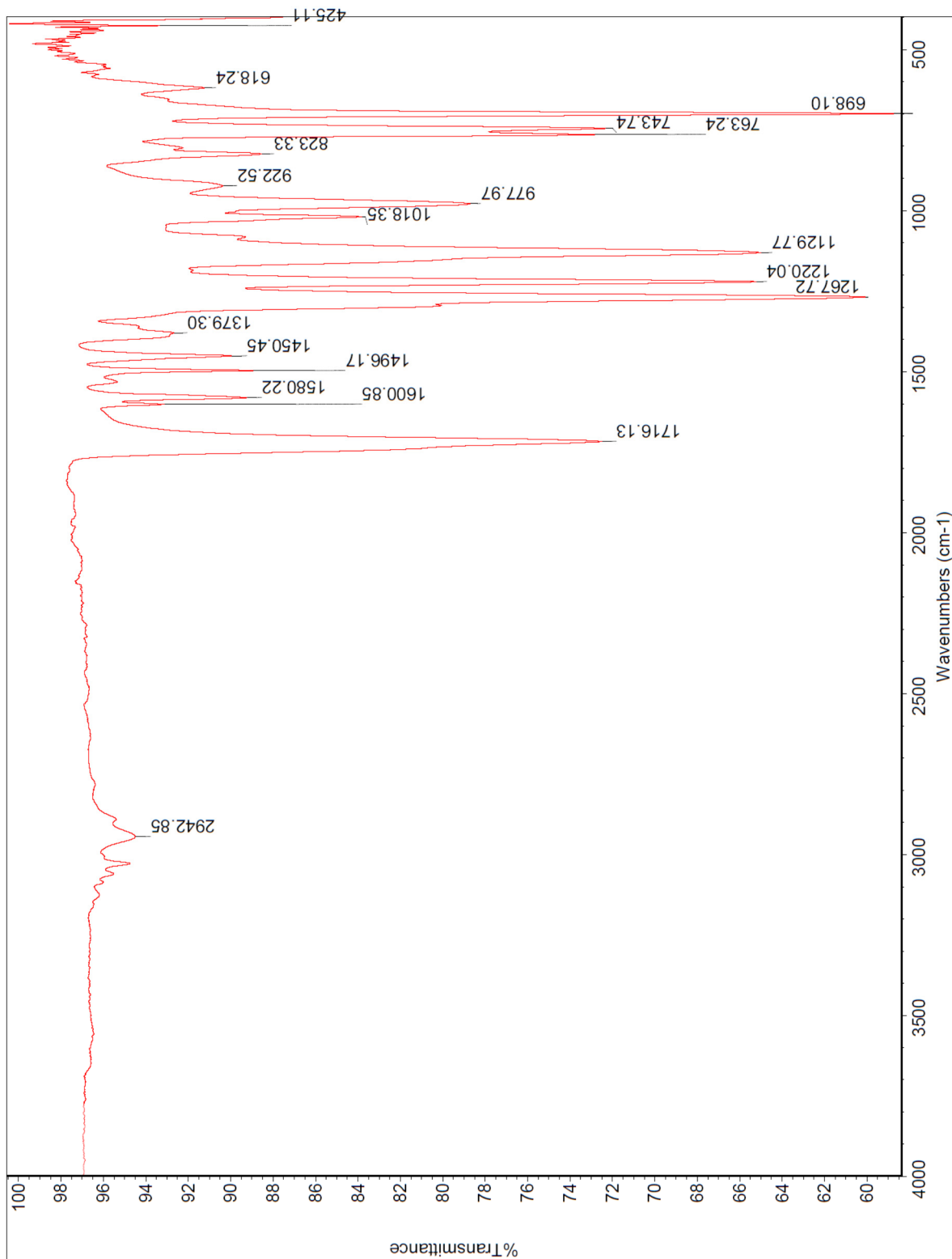


Figure S30. FT-IR spectrum of **PCBF** using ATR detector.

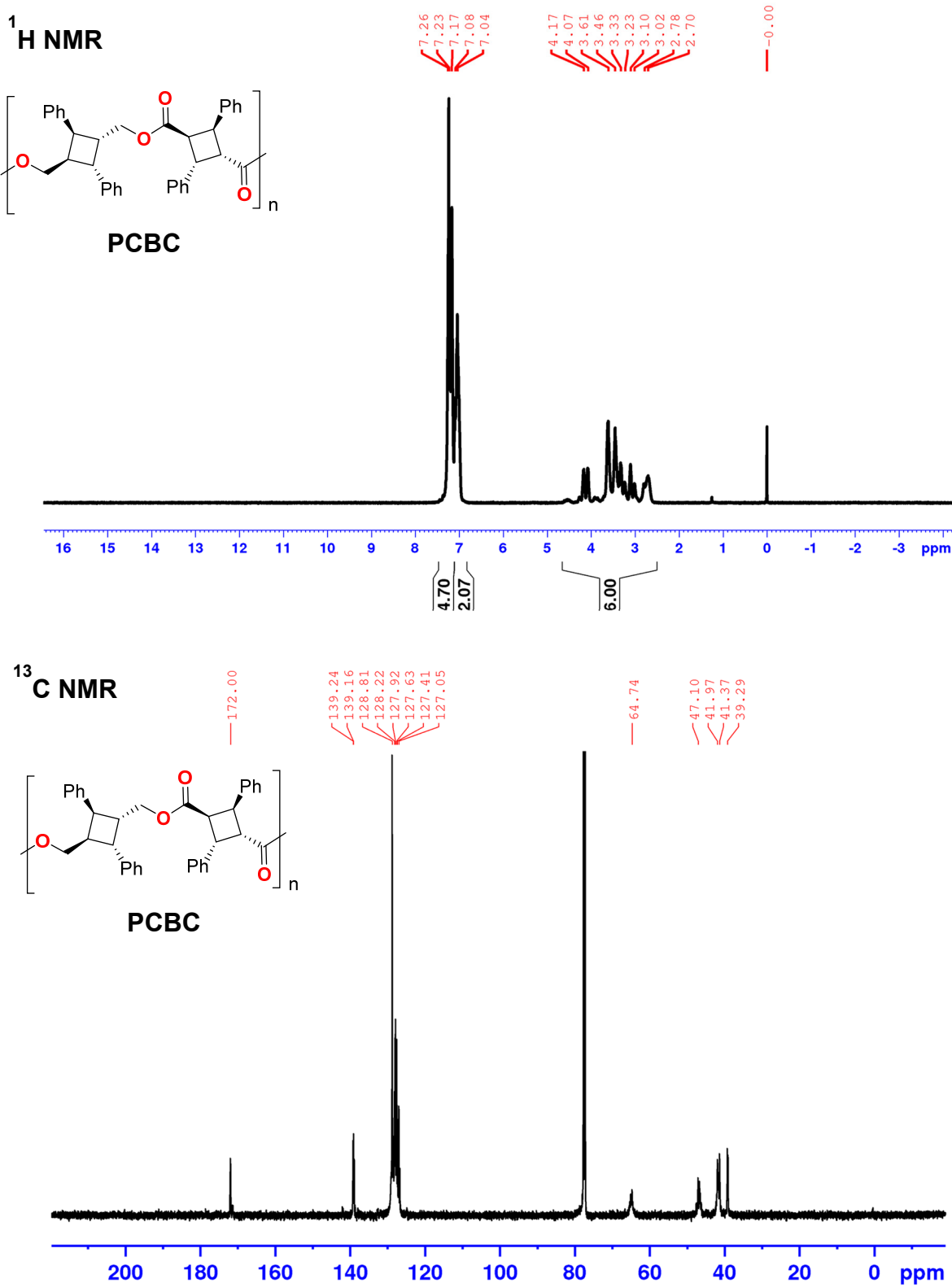


Figure S31. ^1H and ^{13}C NMR spectra of PCBC in CDCl_3 at room temperature.

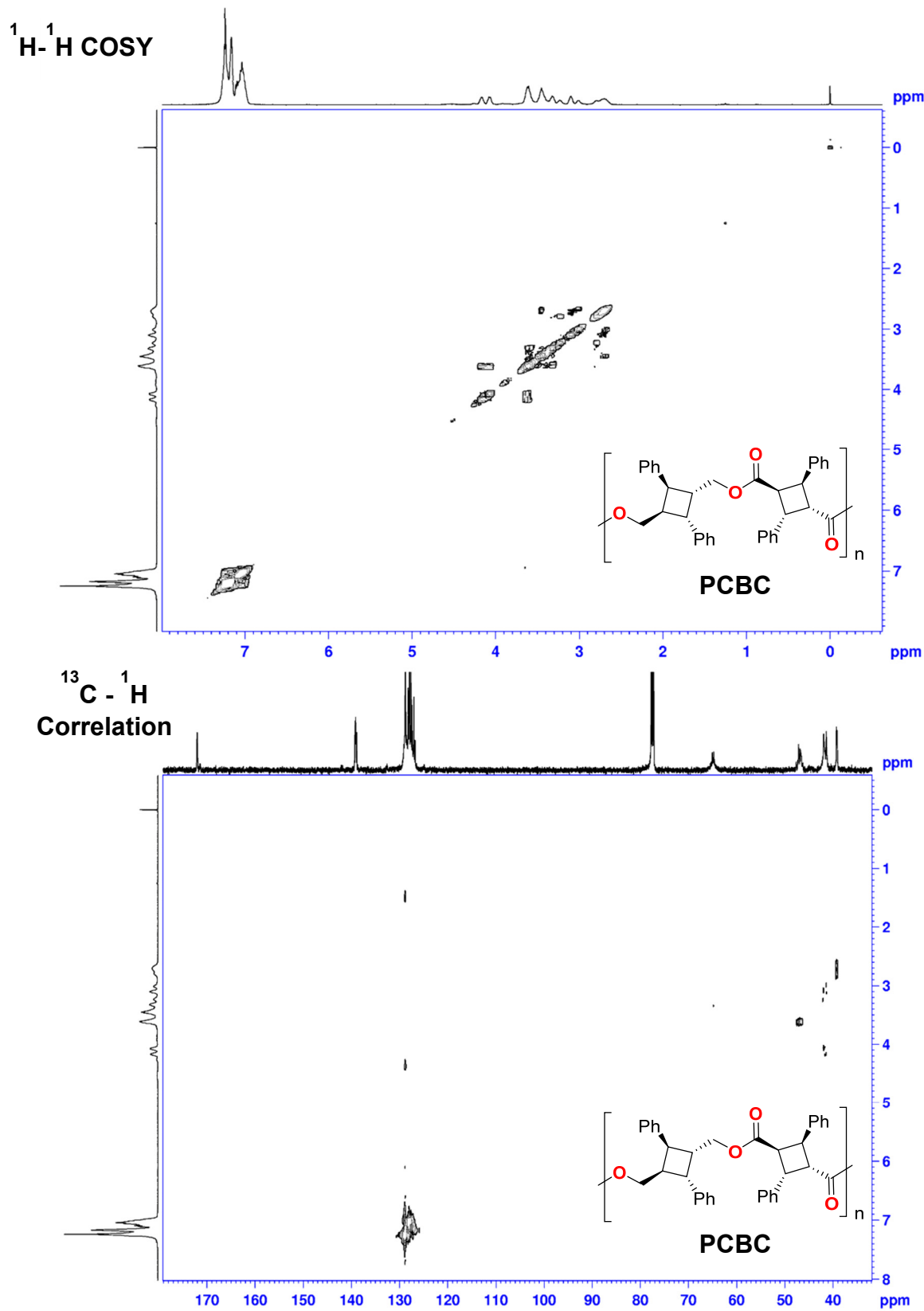


Figure S32.COSY and C-H correlation spectra of PCBC in CDCl_3 at room temperature.

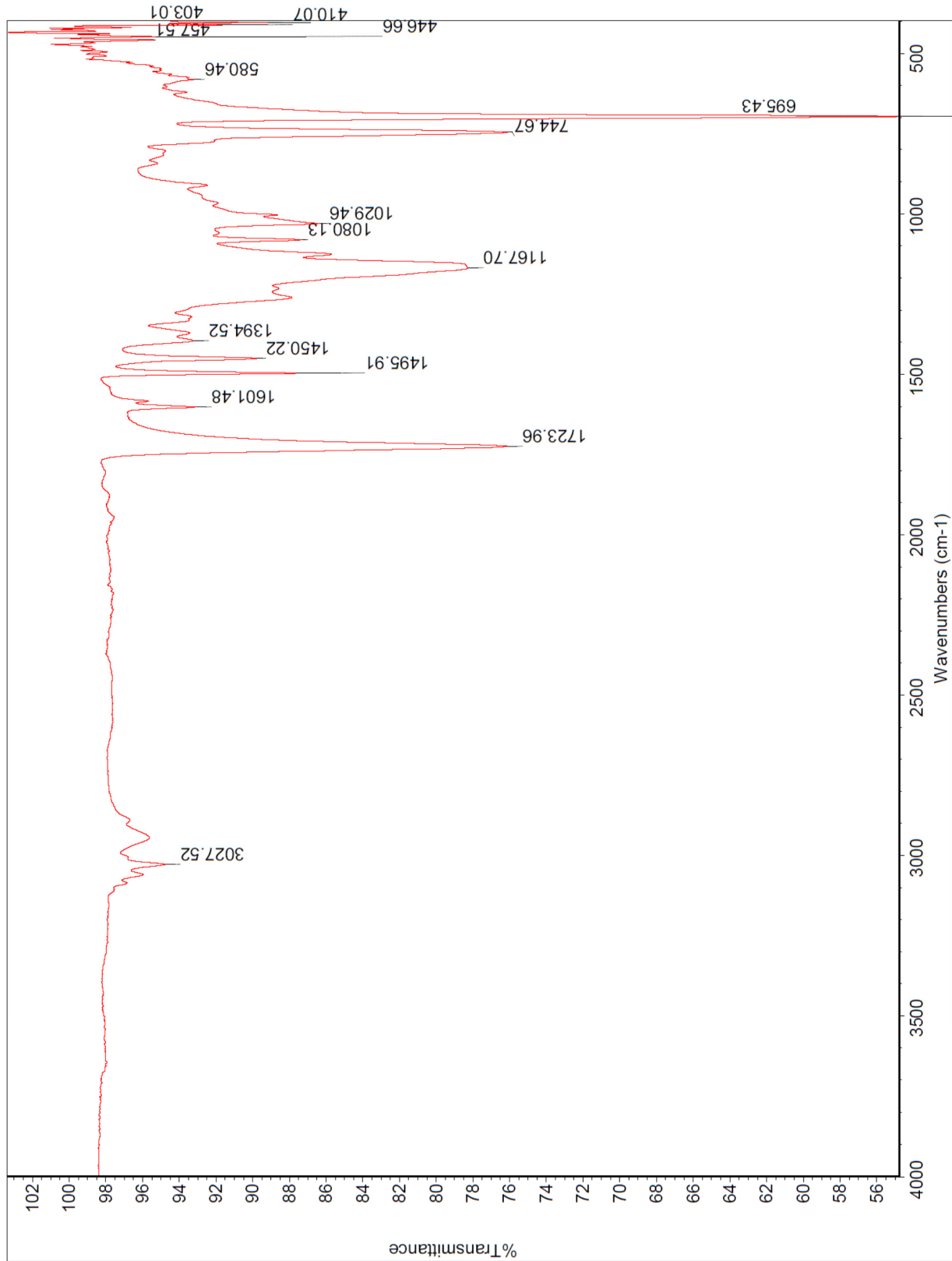
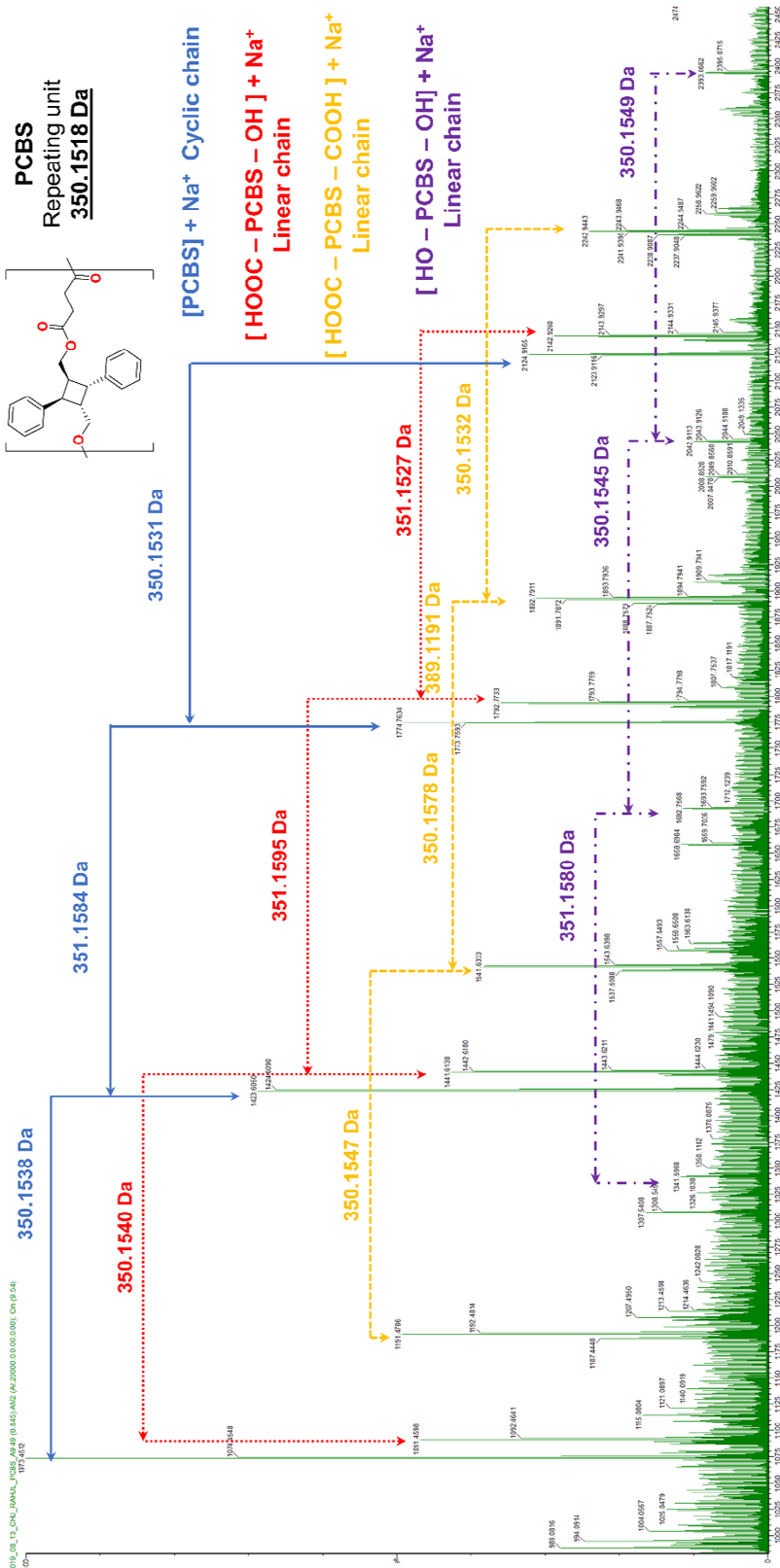


Figure S33. FT-IR spectrum of PCBC using ATR detector.



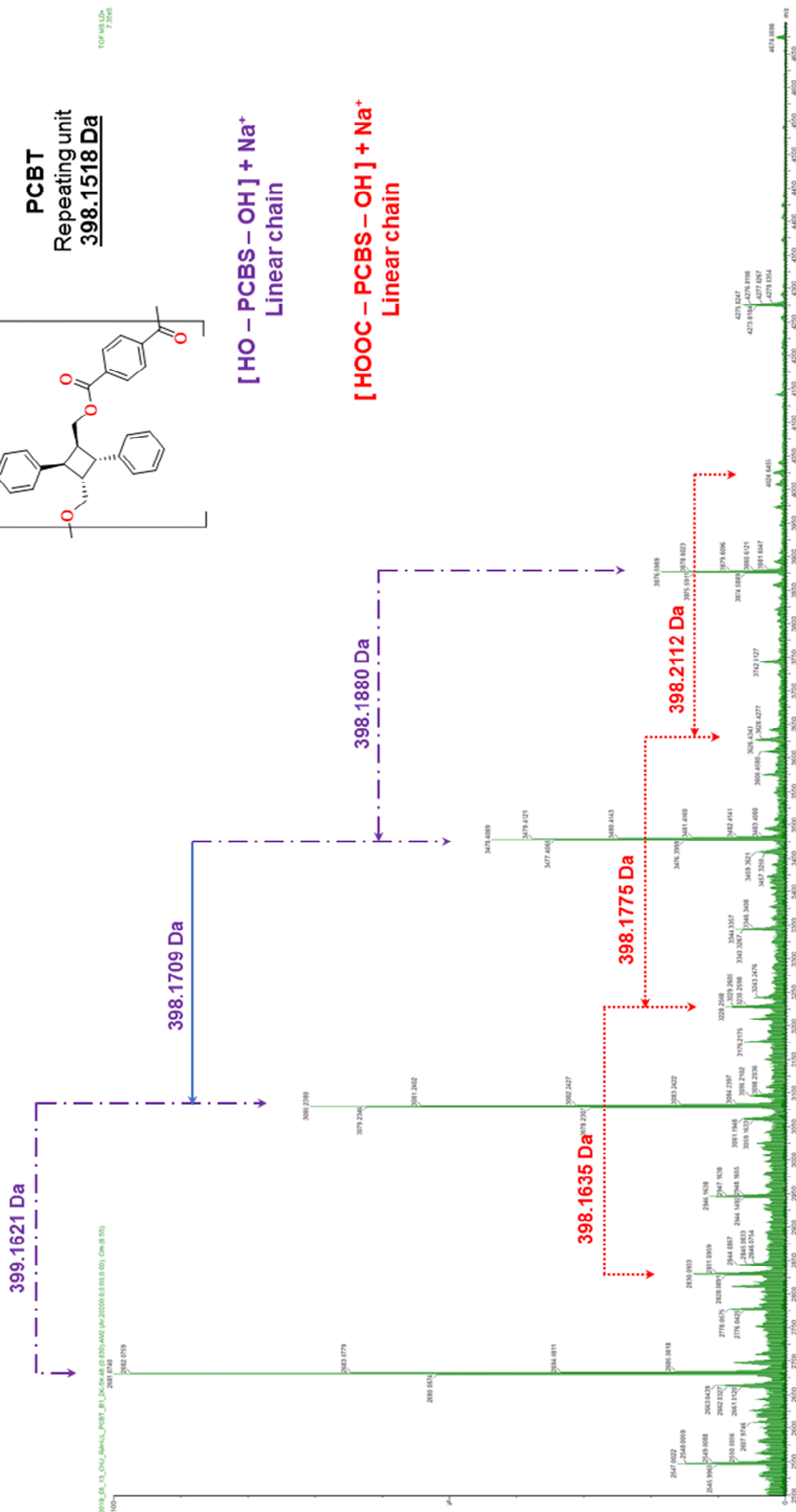


Figure S35. MALDI-TOF-MS spectrum of PCBT.

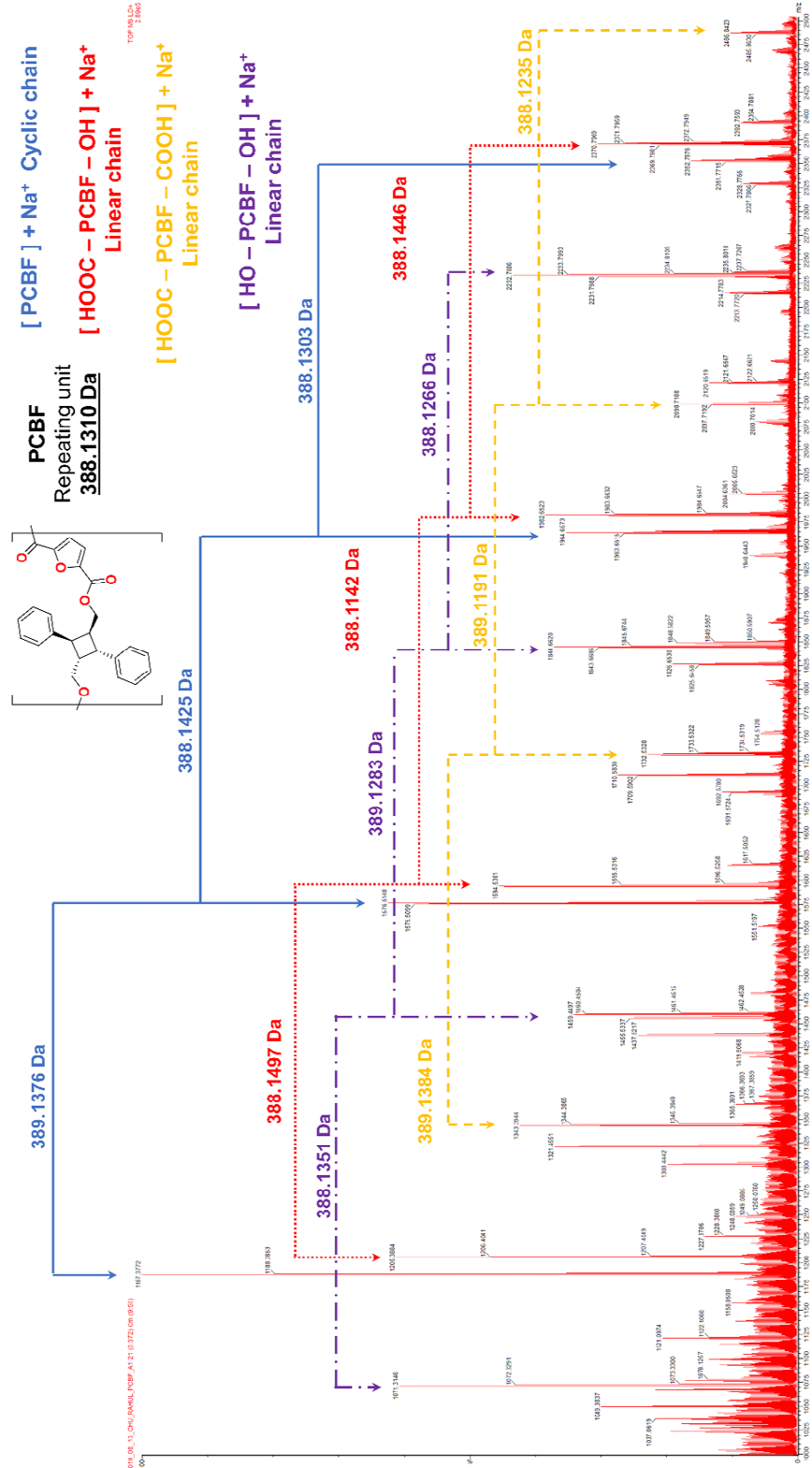


Figure S36. MALDI-TOF-MS spectrum of PCBF.

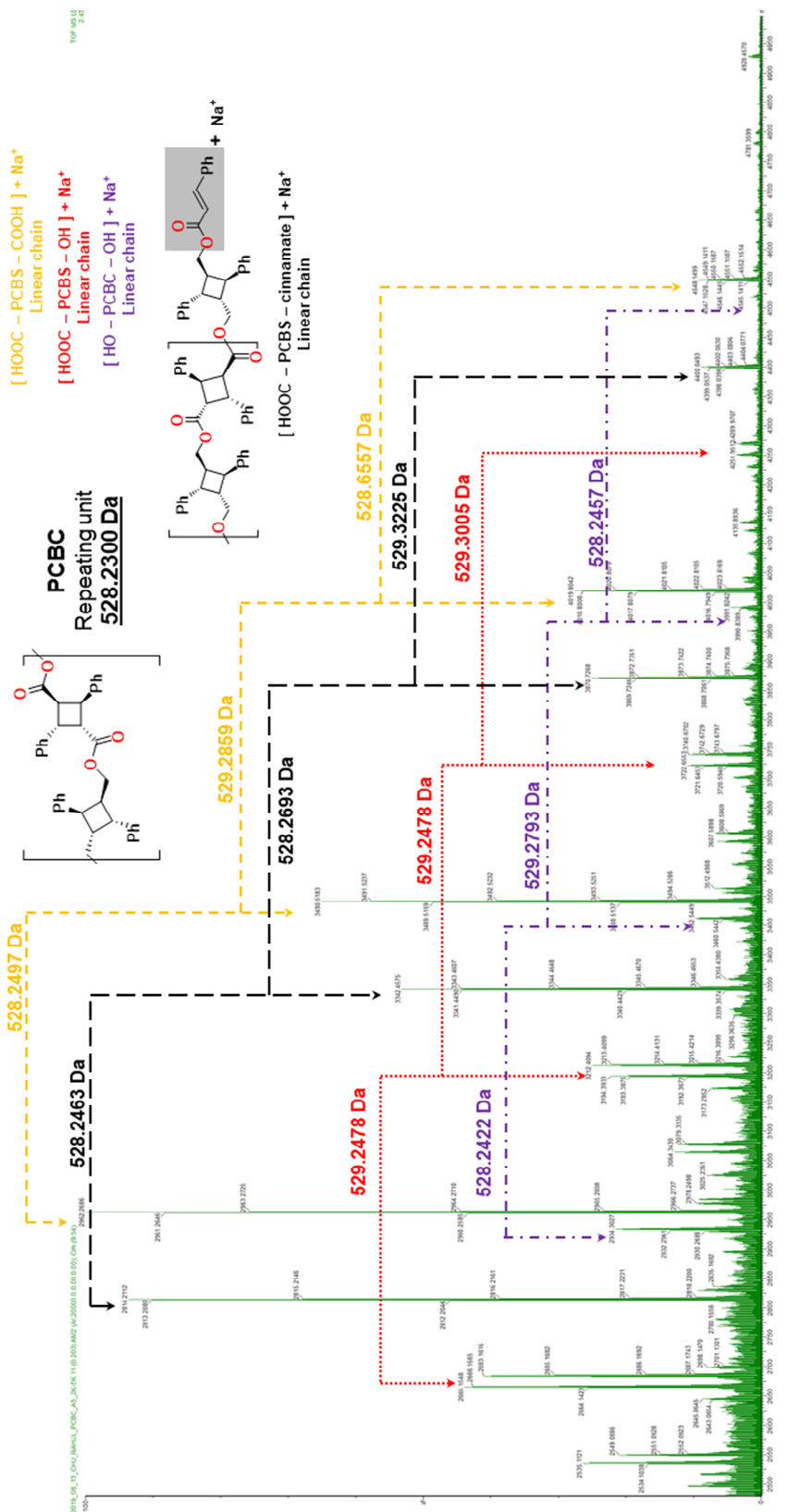


Figure S37. MALDI-TOF-MS spectrum of PCBC.

Table S1. Thermo-physical properties of some known polyesters compared with synthesized Polyesters.

Polyester	Glass Transition Temperature, T _g (°C)
Polyethylene Succinate	-11 to -1
PCBS	53
Polyethylene Adipate	-70 to -40
PCBA	35
Polyethylene Terephthalate	64 to 84
PCBT	114
Polyethylene Furan 2,5 dicarboxylate	80 to 87
PCBF	109

Table S2. Available commercial polystyrene and poly(methyl methacrylate) standards listed by peak molecular weight (Mp) and retention times obtained on PLgel Minimix-D column with THF as a mobile phase (3 µL injection volume and 0.3 mL/min flow rate).

PS Standards (Mp)	580	1480	2340	5030	8450	19760	38100	70950	132900	271800
Retention Time (min)	9.2	8.8	8.4	8.0	7.7	7.2	6.9	6.5	6.2	6.0
PMMA Standards (Mp)	550	960	1780	2880	4640	6850	10280	17810	26080	56600
Retention Time (min)	9.4	9.3	8.7	8.4	8.1	7.9	7.7	7.4	7.2	6.7

Table S3. Diffusion Coefficient – Molecular weight results of PS calibration curve using DOSY.

Samples	M (g/mol)	D (10^{-10}) (m 2 /s)	logD	logM
PS	1480	6.50 ± 0.02	-9.18709	3.170262
PS	2340	4.98 ± 0.03	-9.30277	3.369216
PS	5030	3.29 ± 0.04	-9.4828	3.701568
PS	8450	2.44 ± 0.01	-9.61261	3.926857
PS	19760	1.53 ± 0.04	-9.81531	4.295787
PS	38100	1.03 ± 0.02	-9.98716	4.580925
PS	70950	0.87 ± 0.01	-10.059	4.850952
PS	132900	0.56 ± 0.01	-10.2472	5.123525

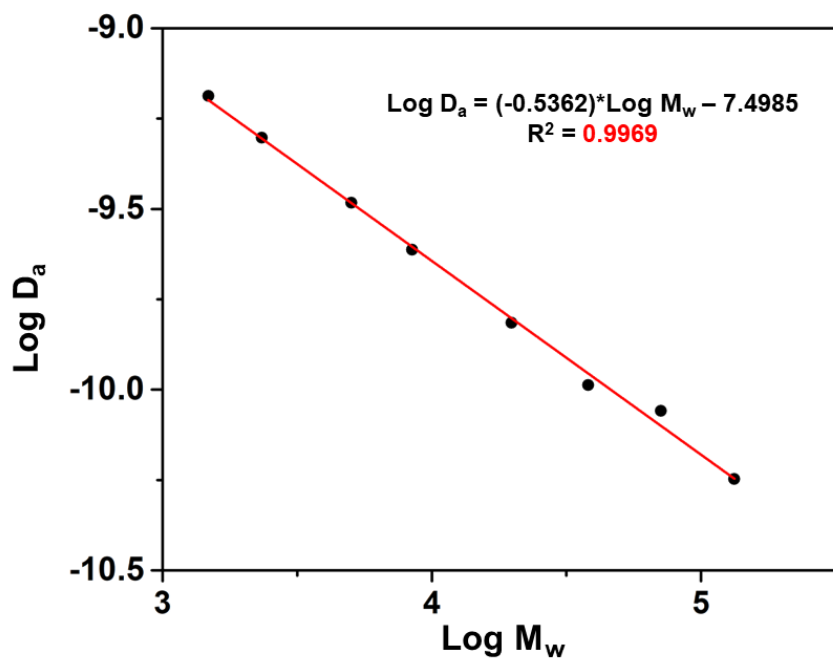


Figure S38. PS calibration curve in CDCl₃ for M_w prediction

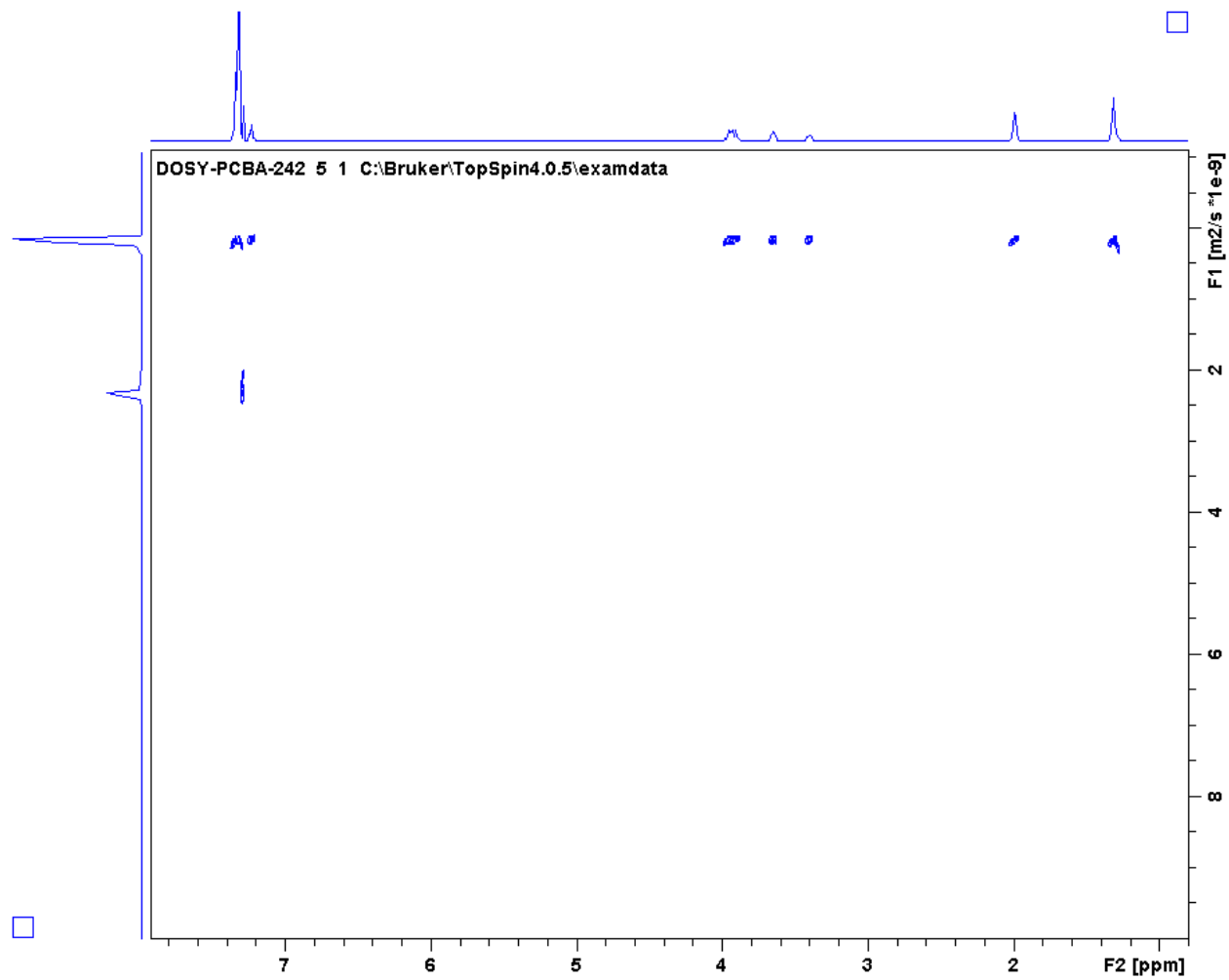


Figure S39. 2D DOSY spectra of PCBA in CDCl₃ for molecular weight calculation

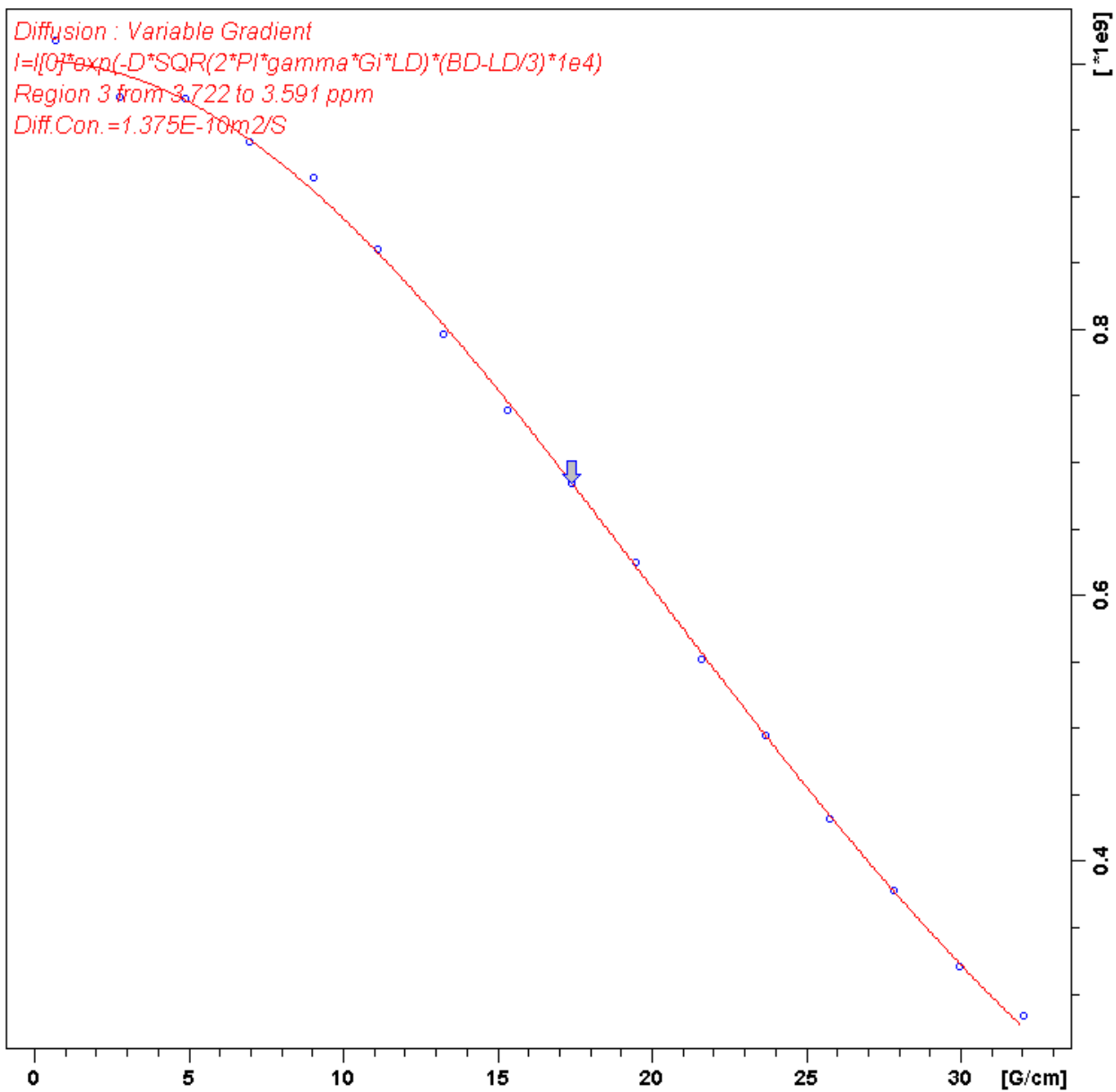


Figure S40. Exemplary signal intensity (Int) decay curve of cyclobutane ring protons (chemical shift = 3.67 ppm) derived from DOSY on a PCBA sample using diffusion time $\Delta = 100$ ms. The data was fitted (—) with the Stejskal-Tanner equation ($I = I_0 \exp(-\gamma^2 g^2 \delta^2 D(\Delta - \delta/3))$) to derive a diffusion coefficient $D = 1.375 \cdot 10^{-11}$, which using the PS calibration (Figure S38) resulted in an $M_w = 25,700$ g/mol.